
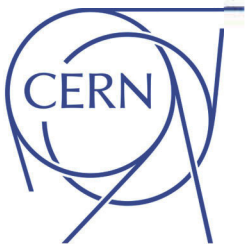


# Time-of-Flight mass separation of charged isotopes with a Bradbury-Nielsen Gate

(Massentrennung geladener Isotope über ihre Flugzeit mithilfe eines Bradbury-Nielsen Gatters)

Bachelor Thesis of

Eleni Ganzke

at the Department of Physics
Institute of Experimental Particle Physics (ETP)



Supervisor: Dr. Erich Leistenschneider
Reviewer: Prof. Dr. Günter Quast
Second Reviewer: Dr. Stephan Malbrunot-Ettenauer

Karlsruhe, August 21st 2023

## Erklärung:

Ich versichere wahrheitsgemäß, die Arbeit selbstständig verfasst, alle benutzten Hilfsmittel vollständig und genau angegeben und alles kenntlich gemacht zu haben, was aus Arbeiten anderer unverändert oder mit Abänderungen entnommen wurde sowie die Satzung des KIT zur Sicherung guter wissenschaftlicher Praxis in der Fassung vom [Datum] beachtet zu haben.

Ort, Datum

Unterschrift

## Acknowledgement

First of all, I would like to thank everyone who made this work possible for their help and support. I am grateful for the opportunity to complete my undergraduate thesis at MIRACLS and for the opportunity to work in an international research environment like CERN. I learned a lot while I was there, both personally and scientifically.

Above all, I would like to thank my supervisor Erich Leistenschneider who was always available for questions and discussions. I appreciate your help, explanations, and feedback during and after my CERN stay.

Many thanks to Stephan Malbrunot-Ettenauer and Prof. Quast for making my CERN stay and this thesis possible. Thank you, Stephan, for organizing and funding my stay and for your overall support! Many thanks to my university supervisor Prof. Quast who encouraged me to do this thesis and coordinated all the details involved.

I would like to thank the whole MIRACLS collaboration for such a great working environment. Especially, I would like to thank Franziska Maier for laying the foundation for the simulations in this thesis and for introducing new concepts to me.

Lastly, I would like to thank my family and friends for their encouragements and their mental support.

**Abstract**

The MIRACLS collaboration is working towards building a new experiment that will push the sensitivity of electron affinity measurements. Exceeding the sensitivity limit will provide new stringent tests for atomic theory models of multi-electron systems. MIRACLS' initial experiment aims to measure the isotope shift in the electron affinity between stable chlorine isotopes. To achieve that, it is necessary to separate stable chlorine isotopes to 99% purity.

For this purpose, an ion beam gate is required that selects ion bunches by their different flight times. A Bradbury-Nielsen gate is the chosen approach as it enables a sharp and fast selection with little impact on the selected ion's motion. However, it requires a complex and precise construction. This thesis demonstrates a way to make this process easier and faster while using accessible materials.

The assembled gate is installed in MIRACLS high vacuum setup and exceeds the target performances regarding purification. Lastly, recommendations to further improve its performance in the future are provided as well.

# Contents

# 1 MIRACLS' negative ion project

## 1.1 Motivation to study negative ions

A negative ion is a negatively charged atom or molecule with one or more additional bound electrons. The atomic structure and thus the behavior of negative ions differs significantly from neutral atoms and positive ions [1]. This is caused by the dominance of different forces in binding the outermost electron [1]. For neutral atoms and positive ions, the long-distance Coulomb interaction between the positively charged nucleus and the outermost electron dominates the bonding process. In case of negative ions, the interaction of electrons with each other has a significant impact on the binding force. [1]

In an atom, the outermost electron is relatively strongly attracted to the nucleus as the Coulomb potential is inversely proportional to the distance, r, to the nucleus. The $\frac{1}{r}$-potential in a neutral atom is far-reaching and strong enough to enable an infinite spectrum of excited bound states that converge to the ionization energy as shown in figure 1. For negative ions, the surrounding electrons effectively shield the attractive Coulomb potential of the nucleus. Thus, the outermost electron is bound due to an induced dipole polarization potential of the nucleus proportional to $\frac{1}{r^4}$. As a result, in contrast to the stronger Coulomb potential from the nucleus in atoms, this attractive potential becomes relatively weak with increasing distance from the nucleus, and can typically only produce a single bound state, if any (for comparison, see figure 1).

Negative ions represent an environment in which electron correlations make the decisive contribution to the cohesion of the system and thus are fundamentally different systems from their corresponding neutral atoms. The models that accurately describe the latter cannot be easily applied to the former and vice versa. This is precisely the reason for studying negative ions. A greater understanding of many-electron systems can result from precise measurements of their properties, such as electron affinity, which is the energy released when an electron is added to the atomic structure of a neutral atom. So, the theoretical predictions of such models can be tested experimentally. The different atomic structure of an atom A and its corresponding negative ion $A^-$ can be seen in the energy diagram in figure 1. The electron affinity can also be extracted from this diagram as the difference between the ground states of $A^-$ and A.

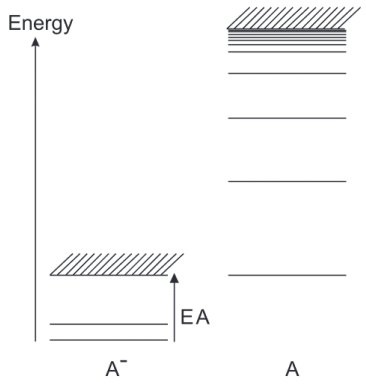


**Figure 1:** Energy level diagram for electrons in a negative ion $A^-$ and in its corresponding atom A: A has an infinite spectrum of excited bound states that converge towards the ionization limit, while $A^-$ has only a single excited bound state. The electron affinity (EA) of A is equal to the energy difference between the ground states of $A^-$ and A and is here indicated as an arrow from the ground state of $A^-$ to the detachment threshold. Figure taken from [2].

[1] The content of this section is discussed in textbooks such as [1] or summaries of the topic such as [2] in greater detail.

## 1.2 The significance of high-precision electron affinity studies

Due to electron-electron interactions, multi-electron systems, in general, cannot be described analytically, resulting in high demand for accurate numerical models. However, these complex calculations are computationally costly and therefore require rigorous experimental tests to determine whether their approaches and approximations are justified and can in fact accurately describe the system. Hereby, the mutual interplay of theory and experiment is critical to obtain the most accurate description possible.

When discussing atomic theory, the nucleus is often simplified as an infinitely heavy point charge. For a description of an atomic model with high precision, these assumptions are not valid anymore, especially when studying the effect of small changes in the overall system. This is the case for studying atoms that have the same amount of protons but different amounts of neutrons in their nucleus. Those atoms are called isotopes. The difference in mass, size, and electric charge distribution between two isotopic nuclei shifts the levels in the atomic energy spectrum relative to each other which then leads to energy shifts in the optical transitions of different isotopes [3]. These minute energy shifts are called isotope shifts. During a radiative transition in atom A, a photon with frequency $\nu_{\mathrm{A}}$ is either absorbed or emitted. The photon energy $h\nu_{\mathrm{A}}$ with h being the Planck constant is the energy difference of the upper and lower atomic level, $\Delta E_{\mathrm{A}}$:

$$\Delta E_{\mathrm{A}} = h\nu_{\mathrm{A}}, \tag{1}$$

From this follows that for two different isotopes A and A' the isotope shift, IS, can be written as follows:

$$IS = \Delta E_{\mathrm{A}} - \Delta E_{\mathrm{A'}} = h\delta\nu_{\mathrm{A,A'}}, \tag{2}$$

where $\delta\nu_{\mathrm{A,A'}}$ is the difference in photon frequency for the same radiative transition once for isotope A and the other time for isotope A'. To a good approximation, the isotopic shift depends only on mass and volume (or field) effects and can therefore be written as follows:

$$\delta\nu_{\mathrm{IS}}^{\mathrm{A,A'}} = \delta\nu_{\mathrm{mass}}^{\mathrm{A,A'}} + \delta\nu_{\mathrm{field}}^{\mathrm{A,A'}}, \tag{3}$$

where $\delta\nu_{mass}^{\mathrm{A,A'}}$ is the mass shift and $\delta\nu_{field}^{\mathrm{A,A'}}$ is the field shift [3]. The so-called normal mass shift is relatively easy to calculate as it arises from the difference in the reduced mass of the electron-nucleus system [4]. However, in many-electron systems, a deviation from this calculated value by the amount of the so-called specific mass shift is observed [4]. This deviation is generally induced by electron correlations. If the specific mass shift can be measured precisely, complex theoretical models and calculations can be tested (see [5] for further details).

As explained in the previous section 1.1 negative ions are excellent probes for studying electron correlation effects and thus testing the validation of atomic theories. However, for negative ions, the electron affinity is the only property that can be measured with high precision [6]. Because isotope shifts in electron affinity are further impacted by electron correlations, precise measurements of isotope shifts in the electron affinity can provide an even better benchmark for theoretical predictions.

## 1.3 High-precision electron affinity studies with photodetachment threshold spectroscopy

The general approach to measure the electron affinity consists of measuring the required energy to detach the outermost electron of a negative ion from the atomic core. If the absorption of a photon initiates this process, it is referred to as photodetachment. Photodetachment is only possible if the photon energy $h\nu$ is at least equal to the electron affinity, in other words the photodetachment

threshold energy. Thus, photodetachment can be seen as a transition from the bound ground state of the negative ion $A^-$ into a continuum state consisting of the residual atom A and the free electron:

$$h\nu + A^- \rightarrow A + \epsilon^-. \tag{4}$$

Because of a very low photodetachment probability around the threshold, the data taken closest to it has the worst signal-to-noise ratio. To fit all the measured data near the threshold region, a theoretical expression for the cross section dependent on the photon energy is needed. In 1948, Wigner derived general expressions for the near-threshold cross sections for different types of processes and shows that the cross section of interacting particles only depends on the long-range interaction between the product particles, no matter the reaction mechanism [7]. The premise for this is that at large distances of the particles, the interaction potential does not go faster to zero than $r^{-2}$ [7]. As for photodetachment, the repulsive centrifugal potential $\frac{l(l+1)}{2 \cdot r^2}$ with l being the orbital angular momentum quantum number is the dominating potential for long-range interaction as the dipole polarization potential goes faster to zero than $r^{-2}$. Thus, the cross section $\sigma$ can be described with the following expression according to Wigner [7] with k being the linear momentum and l being the orbital angular momentum of the detached electron:

$$\sigma \sim k^{2l+1}. \tag{5}$$

This relation can be rewritten in terms of energy by making use of the energy conservation $h\nu = \mathrm{EA} + \frac{\hbar^2 k^2}{2m}$ in the photodetachment process with m being the electron mass, EA being the electron affinity which is the same as the threshold energy $E_{\mathrm{thr}}$ and $E_{\mathrm{ph}} = h\nu$ being the photon energy which is directly proportional to its frequency $\nu$ :

$$\sigma(E) \sim (E_{\mathrm{ph}} - E_{\mathrm{thr}})^{l+1/2}. \tag{6}$$

This relationship between the cross section and photon energy is known as the Wigner law. In principle, the neglect of shorter-range interactions in Wigner's law limits the range of validity for the Wigner law [1]. However, it does not affect the form of the threshold [8].

When the electron transitions from its former bound state with the angular momentum quantum number $l_0$ to its final state with angular momentum $l$, the only allowed values for this quantum number in the final state are $l = l_0 \pm 1$ because of the electric dipole selection rules. So, bound electrons in an s-state ($l_0 = 0$) will be emitted as a p-wave, meaning with $l = 1$ in their final state. According to Wigner's law, the cross section near the threshold follows a slow onset with $\sigma \sim E^{\frac{3}{2}}$ which is shown in figure 2. Detached electrons from a bound state with $l_0 > 0$ need to tunnel through a potential barrier caused by the interplay of the repulsive centrifugal potential and the attractive dipole polarization potential. This barrier strongly suppresses the $l = l_0 + 1$-emission relatively to one with $l = l_0 - 1$ [2]. Thus, an electron detached from a p-state will be emitted as an s-wave with $l = 0$. As shown in figure 2, this leads to a sharp onset for the cross section near the threshold which improves the precision of electron affinity measurements.

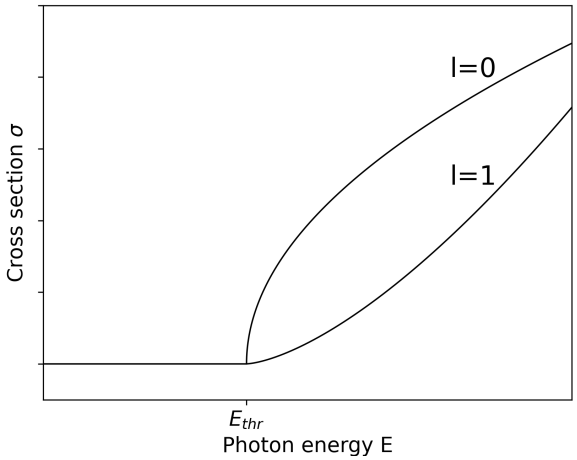


**Figure 2:** The behavior of cross section around the threshold region as a function of photon energy according to Wigner law for a photodetachment process is illustrated: Depending on the angular momentum quantum number l of the emitted electron, the cross section follows a different form for energies above the threshold energy. For $l = 0$ (s-wave) the cross section follows a $E^{\frac{1}{2}}$- and for $l = 1$ a $E^{\frac{3}{2}}$- behaviour. For photon energies below the threshold, the cross section remains zero.

Since the data closest to the threshold energy has the lowest signal-to-noise ratio, expanding the data set available for evaluating the threshold energy is critical. This is accomplished by fitting the data to the Wigner function and then extrapolating to the threshold. The sharp onset of the cross section at the threshold energy allows for high precision in determining the electron affinity.

The chosen measurement technique is laser photodetachment threshold spectroscopy (LPT), because it is not only a precise technique for studying electron affinities, but also a very sensitive technique. This is demonstrated by previous experiments such as Berzinsh et al.'s which outperforms the sensitivity of previous electron affinity measurements by a factor of two [6].

## 1.4 Higher sensitivity boost needed for isotope shifts in the electron affinity

As previously argued in section 1.2, isotope shifts in the electron affinity (IS-EA) are good tests for atomic theories. However, IS-EA have been measured only in a couple of cases due to technical constraints. This is because the shifts are small and the cross section at the level necessary to see their differences is minute. As a result, the signal-to-noise is not enough to distinguish small shifts. Thus, there is a need to boost the signal which cannot be achieved with conventional laser photodetachment threshold spectroscopy.

## 1.5 MIRACLS superior technique for boosting sensitivity

In conventional collinear laser photodetachment threshold spectroscopy, an ion beam is collinearly overlapped with a laser beam to maximize the interaction length and hence the probability of excitation. MIRACLS seeks to further increase the interaction time between laser and ion beam. To achieve this, ions are trapped in a Multi Reflection Time-of-Flight (MR-ToF) device. The ion beam is trapped when the MR-ToF switches its two coaxial electrostatic mirrors to a higher potential so that the ions cannot escape. They are trapped inside a drift tube and are passing the optical detection region for multiple revolutions. This can boost the signal sensitivity by orders of magnitudes compared to a single-pass experiments.

In figure 3 the MIRACLS setup of the negative ion project is shown. A continuous ion beam of the isotopes $^{35}$Cl and $^{37}$Cl is trapped in a linear Paul trap filled with Helium as buffer gas. In the Paul trap, the ions are cooled and bunched in ion packages. After a certain amount of time, such an ion package which consists ideally of roughly 1000 ions is emitted by the Paul trap. After that, the ion bunch is accelerated by a voltage U into a drift tube, where the isotopes separate due to their difference in mass. The ion beam overlaps with a laser beam as shown in red (ion beam) and blue (laser beam) in the lower part of figure 3. The laser frequency is scanned across the threshold region of detachment and the resulting neutral Cl atoms are detected by the MagneToF detector shown in figure 3.

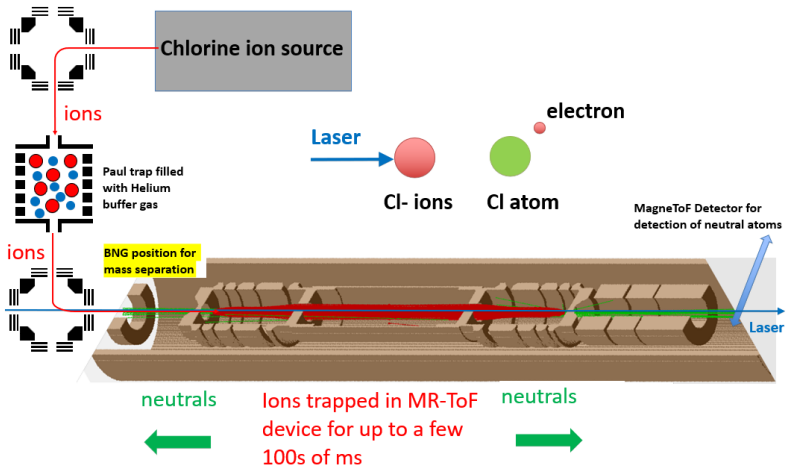


**Figure 3:** Schematic overview of the MIRACLS setup. Figure adapted from [9].

## 1.6 Motivation for studying the isotope shift between $^{35}$Cl and $^{37}$Cl

The isotope shift in the electron affinity between $^{35}$Cl and $^{37}$Cl, in particular, needs to be determined experimentally with higher precision than it is presently. This is because Carette's and Godefroid's theoretical calculation [10] is more precise than Berzinsh et al.'s experimentally determined isotope shift [6]. Consequently, an experimental determination of higher precision would test the validity of Carette's and Godefroid's calculations [10] which is exactly the goal of MIRACLS negative ion project. This can be achieved with narrow-band continuous-wave lasers [9] which due to their limited laser power have not been used in previous experiments to determine the isotope shift in the electron affinity between $^{35}$Cl and $^{37}$Cl. Due to the high increase in sensitivity described in section 1.5 these lasers can be used in the MIRACLS' setup and therefore a higher precision is

expected from the MIRACLS experiment.

## 1.7 Motivation for installing a Bradbury-Nielsen gate into the MIRACLS setup

For precisely determining the energy shift in the electron affinity between $^{35}$Cl and $^{37}$Cl, it is essential to measure each isotope on its own, thus, manipulating the ion beam so that only one isotope can enter the MR-ToF device. A fast solution was to use an electrode steerer configuration to deflect the not-selected ion bunch when the two ion bunches are separated enough due to their flight times. However, the large deflection area induces uncontrolled energy shifts between the isotopes. To improve the isotope selection process the installation of a Bradbury-Nielsen gate (BNG) is the proposed solution. A BNG allows faster ion selection because its electric field decays rapidly with distance from the BNG plane [11]. Therefore, the ions are only exposed to the electric field for a short time, allowing isotope selection with a minor impact on the selected ions' motion. Thus, sharp and defined peaks can be obtained during measurements.

From a technical point of view, the BNG is the preferred selection method as it is simpler to operate and takes up less space than other methods. The infrastructure of the setup (bunched beams, isotope separation based on their flight times) is already in place for a BNG to function effectively (discussed in more detail in section 3).

Magnetic filters are frequently used to separate ions of different masses. Magnetic fields, on the other hand, should be avoided in a precision laser spectroscopy region because they may induce Zeeman shifts. A magnetic filter would be positioned close to this region due to space constraints in the MIRACLS' setup. As a result, magnetic filters are not the best option in this case. They are also unnecessary since the time-of-flight separation in the drift tube provides a sufficient isotope separation, requiring only one deflector device to select the desired isotope. The BNG is the preferred device for this purpose for the reasons stated earlier in this section.

The aim of this work is to assemble and install a working BNG into the MIRACLS' setup so that isotope shifts can be measured in the future. For this reason, this work specifies performance requirements and bases design decisions on them. The assembly is extremely complex and needs a high level of precision. This work demonstrates how to construct an auxiliary device to make this process easier and faster using accessible materials.

# 2 Introduction to a Bradbury-Nielsen gate

A Bradbury-Nielsen gate is an electric gate invented in 1936 by Norris Bradbury and Russell Nielsen [12] for manipulating the trajectory of charged particles. It was developed to study electron mobility in gases, but in recent years it has become more popular for separating ions of different masses based on their flight times [13]. Weinkauf et al. were the first to employ it for ion selection in mass spectrometry in 1989 [14].

The design, which is illustrated in figure 4, is based on the simple idea of placing a grid of equidistant wires perpendicular to the beam axis, with the wires alternating in electrical contact with each other. When a voltage is applied to one set of wires while the other is grounded, the electrostatic field between the wires deflects the ion beam. This effect can be used to prevent the ion beam from entering an apparatus with a small entry. The wires must be thick enough to achieve a large enough deflection angle but also thin enough to have a sufficiently high transmission for ions that should pass through the gate without being deflected. This is discussed in more detail in section 3.

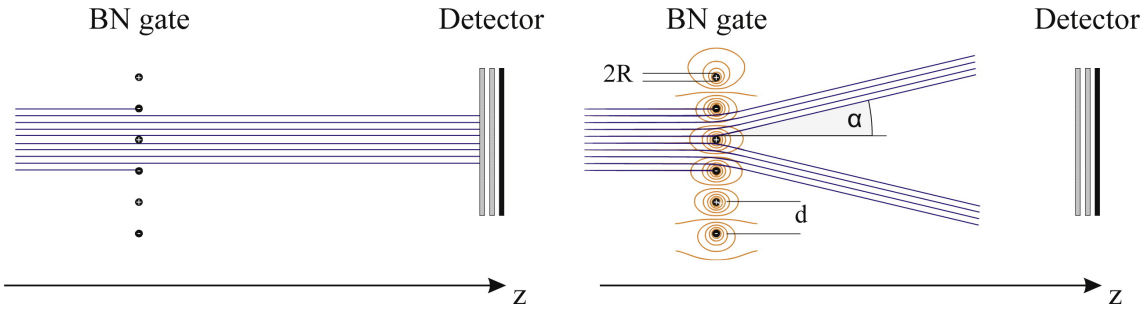


**Figure 4:** Illustration of a BNGs' working principle: If both wire sets are grounded the ion beam is transmitted. If a voltage is applied to one wire set, the ions are deflected. Figure taken from [15].

A BNG is in its transparent state when the ion beam is nearly entirely transmitted; it is in its deflecting state when it deflects the ion beam entirely. When the BNG switches states, it is in a transient state for a short period of time. During this period, it can deflect ions with any angle between 0° and the maximum angle in the deflecting state. To achieve nearly 100% purification, the two ion bunches must be sufficiently separated from each other due to their flight times.

## 2.1 Theoretical model of the BNG

Before designing and assembling the BNG, it is crucial to understand the relationships between the defining quantities such as deflection angle $\alpha$, applied voltage $V_p$ and wire diameter 2R with R being the wire radius. For this reason, this section briefly discusses an analytical model of the electric field induced by a Bradbury-Nielsen gate if the alternating wires are switched to a bipolar potential $\pm V_p$ as demonstrated in figure 5.

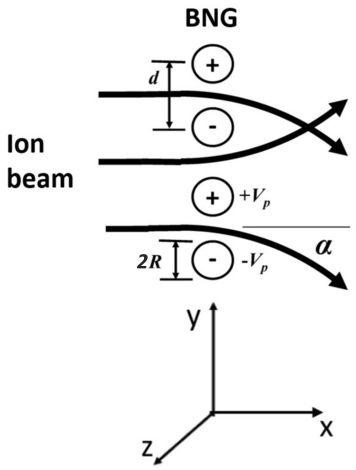


**Figure 5:** Illustration for deriving the expression 7 of the potential surface of a BNG with the wire spacing d and the radius R. Figure adapted and taken from [11].

An analytical expression for the potential energy surface of the BNG was first derived in 1929 by Bethe [16]. According to Yoon, O.K. et al. [17], the expression can be rewritten as follows:

$$U(x,y) = k\frac{V_p}{\pi} \cdot \ln\left[\frac{\cosh\left(\frac{\pi x}{d}\right) - \sin\left(\frac{\pi y}{d}\right)}{\cosh\left(\frac{\pi x}{d}\right) + \sin\left(\frac{\pi y}{d}\right)}\right], \tag{7}$$

where the BNG is in the y-z-plane as in figure 5, with R being the wire radius, d the wire distance (from center-to-center), $\pm V_p$ the voltage applied on the alternating wires and with k being defined as follows:

$$k = \frac{\pi}{2\ln\left[\cot\left(\frac{\pi R}{2d}\right)\right]}. \tag{8}$$

For distances far away from the BNG the deflection angle, $\alpha$, can be approximately determined by the following formula according to Yoon, O.K. et al. [17]:

$$\tan(\alpha) = k\frac{V_p}{V_0}, \tag{9}$$

$V_0$ is hereby the acceleration voltage of the ions. Equation 9 is used to determine the wire diameter and the necessary voltage $V_p$ (see section 3.3) to achieve the desired deflection angle, which is manifested in the following section. Before designing and assembling a BNG, it is essential to conduct a feasibility study first. Since each setup has fixed dimensions and parameters, the performance requirements of a BNG can vary greatly. For example, the ion beam energy strongly influences the deflection angle, or the wire radius cannot be made arbitrarily larger to achieve a bigger deflection angle as the transmission decreases. A feasibility study is carried out in the following section to determine the performance requirements and, thus, properties of the BNG, like the size of the wire radius.

# 3 Feasibility and design study

There are a total of three free parameters for designing and assembling a Bradbury-Nielsen gate that can be modified for the unique performance specifications in a given arrangement. These three factors are the wire diameter, the spacing between adjacent wires, and the applied voltage between the two wire sets. However, the wire spacing was already fixed as an already existing BNG design was adopted from R.N. Wolf et al. [13]. Before integrating the BNG into the setup, it is vital to define the performance requirements for it and thus optimize the dimension of its parameters.

## 3.1 Performance requirements

The beam transmission should be ideally above 90% in the BNG's transparent state, and in its deflecting state, it should be 0%. As a result, the wire has to be thin enough to fulfill the transmission criteria in the transparent state, but at the same time thick enough for a big enough deflection angle to meet the transmission criteria in the deflecting state.

When selecting one isotope, the BNG should not influence the selected ion's motion and achieve above 99% purification at the same time. This means the BNG needs to switch fast enough from its deflecting state to its transparent state and back to the deflecting state.

When determining the position of the BNG with respect to the entire beam line, it is essential to find a balance between sufficient time separation of the ion bunches after the Paul trap and sufficient beam angling before the MR-ToF entrance. In the MIRACLS setup, an actuator is already installed at a position throughout the beamline that can potentially balance both requirements. The following design and feasibility study is performed for this actuating position of the BNG.

## 3.2 Determine the required deflection angle

For a focused beam, a deflection angle of half the MR-ToF opening angle is sufficient to prevent ions from entering and thus also from being registered by the detector. For the dimensions of the MIRACLS setup (distance between BNG and MR-Tof and radius of MR-Tof opening), the calculated deflection angle would be 1.7°. This simple geometric consideration perhaps would be sufficient if the ion beam was indeed focused. However, this is not the case as simulations using the software package SIMION [18] will show in this section. Also, the simulations are supposed to study if the Einzel lenses between the BNG position and the MR-ToF opening affect the required minimal deflection angle.

SIMION is a software package for simulations of electric fields and ion trajectories passing through them. The MIRACLS setup which is described in section 1.5 has been simulated by F. Maier [19]. Based on these existing simulations, which include the setup region shown in figures 6, 8 and 9 and a simulation of the ion beam shown in figure 7, simulations of an ion beam starting at BNG's future position are performed with different initial conditions to determine the required deflection angle (see figures 6, 8, and 9).

Figure 6 shows a simulated focused ion beam deflected in the vertical direction with a 2°-angle which is not entering the apparatus. Thus, a focused beam would behave as it is expected by the geometric calculation. Therefore, the Einzel lenses should only have a negligible influence on the required deflection angle, if any.

**Figure 6:** Simulations of a focused ion beam with a half angle of 0.5° entering the BNG and being deflected with an angle of 2° in the vertical direction. (simulation in analogy to F. Maier [19] using SIMION [18]; simulation of MIRACLS setup done by F. Maier [19] )

However, figure 7 shows simulations on how widely spread the actual ion beam enters the BNG area. Especially on the horizontal axis, the simulated ions distribute over a width of nearly 20 mm.

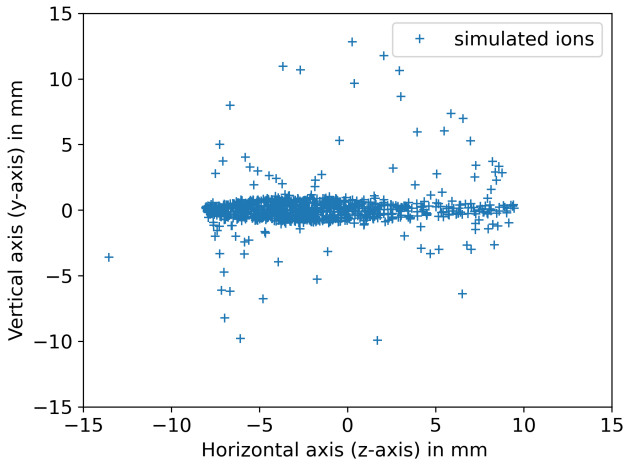


**Figure 7:** Simulation of the ion beam, how it enters the BNG area: ion beam projected on a plane (y-z-plane in figure 5) perpendicular to the direction of propagation (x-direction in figure 5). Ion beam simulated from the Paul trap. Simulation performed by F. Maier [20] using SIMION [18].

Since the BNG deflects the ions at an angle $\alpha$ in the positive and negative direction of the corresponding axis (illustrated in figure 5 along the y-axis), it is more efficient to deflect the ion beam along the vertical axis in figure 7. This requires a smaller deflection angle than deflecting along the horizontal axis as the ions are much more focused around the center in the vertical direction (see figure 7).

The simulation shown in figure 8 illustrates how a deflection angle of 1.7° is too small to prevent ions from entering the apparatus and being trapped inside the MR-ToF device. Figure 9 shows that a deflection angle twice as big (3.4°) is needed to prevent almost all ions from entering the apparatus. Those few that enter cannot be trapped inside the apparatus and thus do not contaminate the measurement of the selected isotope bunch. To conclude, the assembled BNG must be able to deflect an ion bunch with an angle of 3.4°.

**Figure 8:** Simulations of a realistic ion beam entering the BNG and being deflected with an angle of 1.7° in the vertical direction. (Simulation in analogy to F. Maier [19] using SIMION [18]; Simulation of MIRACLS setup and simulation of the ion beam done by F. Maier [19].)

**Figure 9:** Simulations of a realistic ion beam entering the BNG and being deflected with an angle of 3.4° in the vertical direction. (Simulation in analogy to F. Maier [19] using SIMION [18]; Simulation of MIRACLS setup and simulation of the ion beam done by F. Maier [19].)

## 3.3 Determine the required wire diameter

Of the originally three free parameters, one is already fixed as the BNG design was provided by R.N. Wolf et al. [13] with a given wire spacing of 0.5 mm. The two remaining parameters are the wire diameter and the applied voltage between the wires. To prevent sparking between the wires and potentially damaging the BNG, the voltage difference between the wires should not exceed 500 V [13]. This operation condition is used to guide the determination of the wire diameter in the following.

The wire thickness reduces the area available for the ions to pass through the BNG plane. Thus, the theoretical transmission T of the BNG in its transparent state can be written as a function of the wire radius R with the fixed wire spacing d:

$$T(R) = \frac{d - 2R}{d}. \tag{10}$$

To determine the maximum wire diameter the transmission is plotted as a function of the diameter in figure 10. It shows that the wire diameter should not exceed 50 $\mu$m to achieve the required transmission of 90% in the BNG's transparent state.

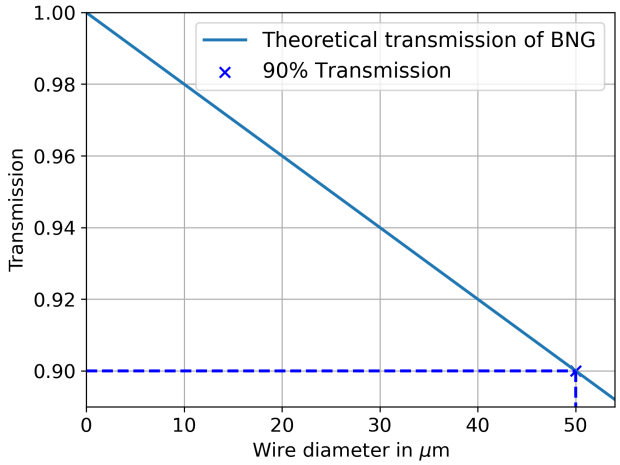


**Figure 10:** Theoretical Transmission of the BNG depending on its wire diameter.

With equation 9 and an approximate ion beam energy of 2215 V which is the transport energy of the ion beam through the setup, the deflection angle is plotted as a function of the absolute voltage applied on each wire set for a fixed 50 $\mu$m diameter (see sub-figure (a) in figure 11). On each wire set, the same absolute voltage is applied but with opposite polarities. For a fixed applied voltage of $\pm$250 V on each wire set the deflection angle is plotted as a function of the wire radius (see sub-figure (b) in figure 11).

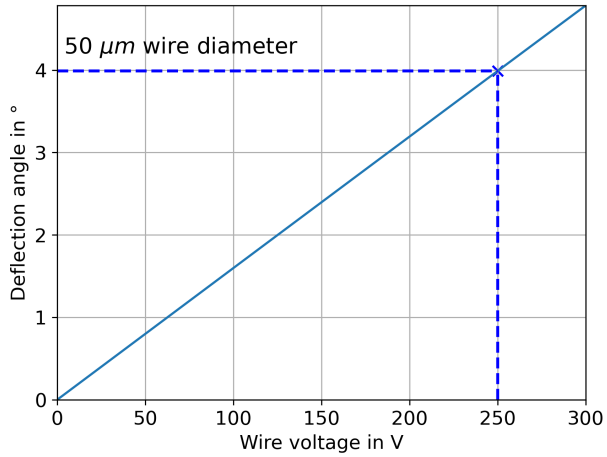


(a) Deflection angle dependent on the absolute voltage applied to each wire set for a fixed wire diameter of 50 $\mu$m. On each wire set, the same absolute voltage value is applied but with opposite polarities.

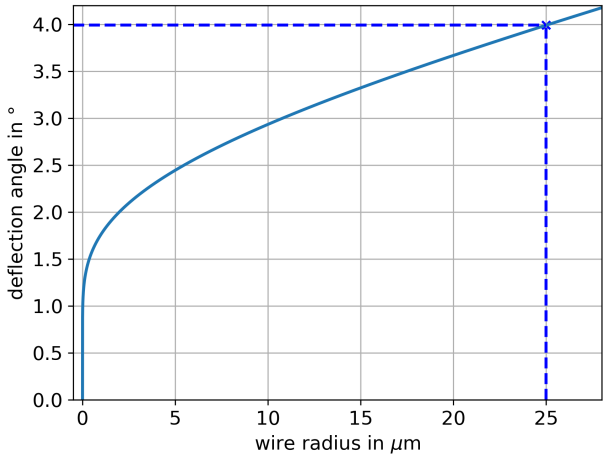


(b) Deflection angle dependent on the wire radius for an applied voltage of $\pm$250 V on each wire set.

**Figure 11:** Deflection angle plotted as a function of the absolute applied voltage on each wire (a) and the wire radius (b). (Both expressions for the plots are derived from equation 9)

It is important to achieve a sufficiently high transmission with 90% as the lower limit but also to have a big enough deflection angle without risking sparking. So, a wire diameter of 50 $\mu$m was chosen for assembling the BNG as it allows 90% transmission and a deflection angle up to 4° without any risk of damaging the BNG. The thinnest possible wire would have been a 35 $\mu$m-diameter

wire. However, considering the gain of an additional 0.5° on the deflection angle and the loosing of just 3% transmission and still fulfilling the 90% transmission requirement, the 50 $\mu$m-diameter wire seems like the better choice. A thicker wire is also more resistant, thus, easier to work with.

## 3.4 BNG's switching conditions for effective isotope separation

The main advantage of a BNG compared to other ion selection methods is that a BNG allows faster ion selection with a minor impact on the selected ions' trajectory. To determine the electron affinity shift between $^{35}$Cl and $^{37}$Cl with high precision, it is crucial to select both isotope ion bunches under the exact same conditions. So, no additional energy shift is created between these two ion bunches. This allows a comparison of the two isotopes without having undesirable effects originating from the ion selection mechanism that could introduce additional uncertainties to the measurement. A symmetric switch that generates a voltage pulse as shown in figure 12, satisfies the above-mentioned requirements since it deflects ions at the opposite edges of the distribution the same way. The two important parameters of the voltage pulse are the time window $\Delta T$ and the voltage magnitude. The preferred value for the voltage magnitude has been defined in the previous section. It is 500 V if the voltage is only applied on one wire set while the other is grounded. The time window $\Delta T$ is defined as the time period when the BNG is in its transparent state (described as 'Gate open' in figure 12).

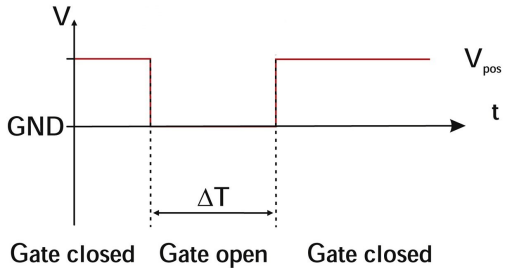


**Figure 12:** Illustration for switching the applied voltage on the BNG: A positive voltage $V_{pos}$ is applied to one wire set and switched to the ground potential for a small time window $\Delta T$. That is when the selected ion bunch passes through the BNG (Gate open). Then it ramps up the voltage again to $V_{pos}$ so that the not-selected ion bunch is deflected. Figure adapted from [15].

To determine the required switching conditions like the time window $\Delta T$ shown in figure 12, it is essential to find out how the isotopes are distributed when they enter the area of the BNG. For instance, the BNG should not switch from transmission to deflection mode while the ion is traveling through the deflection area and yet it should still switch fast enough to effectively separate the ion bunches.

To inspect such timing requirements, a timing detector is positioned where the BNG is to be installed later. The arrival time of each ion bunch after being released from the Paul trap is registered. Both ion bunches are released from the Paul trap at the same time and are accelerated by the same voltage into the drift tube. Thus, both isotope ion bunches have the same constant kinetic energy in the drift tube. This separates the two different isotopes along the drift tube due to their different masses. Because lighter ions travel at higher velocities, the first peak in time registered by the detector can be identified as $^{35}$Cl and the second as $^{37}$Cl. The measured isotope distribution is shown in figure 13.

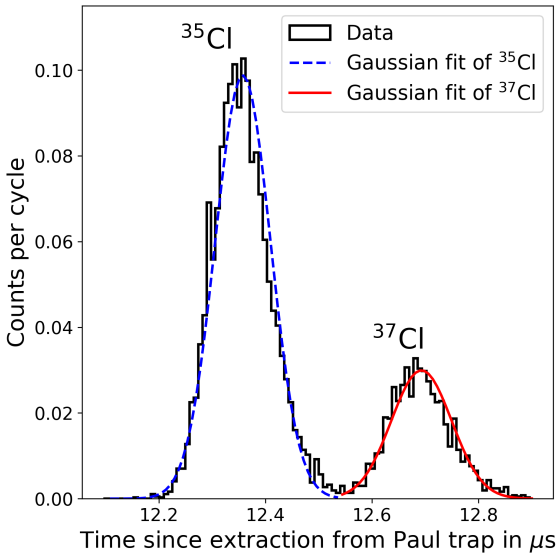


**Figure 13:** Timing profile of $Cl^-$ ion bunches measured by a timing detector installed at the BNG's position.

Each of the ion distributions shown in figure 13 is fitted with a Gaussian function. Table 1 shows the center and the Full width at half maximum (FWHM) of the two Gaussian fits.

**Table 1:** Gaussian fit parameters for the fitted $^{35}$Cl and $^{37}$Cl time-of-flight distribution shwon in figure 13: The average time of flight of ions from Paul trap to BNG is equal to the peak center.

| Isotopes | Center in ns | FWHM in ns |
|---|---|---|
| $^{35}$Cl | $12357.68 \pm 0.92$ | $122.55 \pm 2.63$ |
| $^{37}$Cl | $12692.90 \pm 1.63$ | $133.55 \pm 4.70$ |

Since contamination of up to 1% of the not-selected isotope is still tolerable, a maximally long time window $\Delta T$ was calculated for each isotope distribution in order to let it pass through the gate without being deflected. For this, the approach is to determine the time window $\Delta T$ for which the area of the one Gaussian fit is equal to 1% of the other and vice versa. The time window $\Delta T$ is symmetric to the peak center of the selected isotope. The results are shown in table 2. As both ion bunches have similar FWHM, the shorter time window of 390 ns is chosen. Thus, for effectively separating the two ion bunches, a switch is required, which is able to output such fast voltage pulses.

**Table 2:** Calculated opening time window $\Delta T$ of the gate for each isotope with only 1% contamination of the not-selected one.

| selected isotope | time window $\Delta T$ |
|---|---|
| $^{35}$Cl | $\approx 470$ ns |
| $^{37}$Cl | $\approx 390$ ns |

The switch should be able to generate a voltage pulse as illustrated in figure 12 with a magnitude of 500 V and a pulse width of 300 ns − 400 ns. However, the switches available in the laboratory can only output a pulse with a minimum width of 800 ns, which is twice as long as the maximum

time window determined in table 2.

An attempt was made to solve this problem using an Arduino Nano. A sufficiently fast pulse can be output by port manipulation. It is also important that the leading edge of a single pulse always occurs at exactly the same time. However, due to Arduino's limited clock speed, these fast pulses could not be controlled in the system. The Arduino should register the leading edge of the actual switching pulse as an input and then output a faster pulse. The Arduino was not able to output the pulse at exactly the same time on each revolution. Therefore, it could not be used in the measurements performed in section 5, since the switching start had to be a fixed and known parameter in order to calibrate other parameters that also characterize the performance of the BNG.

For determining the electron affinity shift between $^{35}$Cl and $^{37}$Cl, it is essential to reduce the time window $\Delta T$ as the two isotope ion bunches have to be cut by the switching pulse in exactly the same way to not create additional energy shifts between those two isotopes. However, commissioning, testing the BNG, and showing its improvement to the setup can be done without this last step of switching with a faster voltage pulse.

# 4 The assembly of the Bradbury-Nielsen gate

## 4.1 BNG's Design

Although the operating principle of a BNG is quite simple, there have been several designs proposed over the years and each design has its own advantages and disadvantages. But all of them have the same goal of making the assembly of this device easier and less time-consuming, see for example Kaia, N. et al. [21], Yoon, O.K. et al. [11], Wolf, R.N. et al. [13] or Brunner, T. et al. [15] for more details.

For this work, a BNG design developed by Wolf, R.N. et al. [13] was used. It is shown in figure 14. The wire is woven onto the Peek frame in one operation. The groove structure, also shown in figure 17, allows separation into two sets of wire (top and bottom). This separation is achieved by cutting the wire on the back of the frame, as shown in figure 14 through the blue and red wire set. To hold the wires in place, two insulating plates with non-conductive, ultra-high vacuum-friendly adhesive are glued to the PEEK frame. Since all wires of a wire set must have the same potential, a copper plate is glued onto the grooves of each wire set with conductive, ultra-high-vacuum-friendly adhesive in order to electrically contact them with each other. A stainless steel shield surrounds the BNG's PEEK frame to prevent beam from being implanted into the insulating structure and charging them up electrically. Charging effects could make the BNG unusable since negatively charged parts of the peek frame would deflect the ions in an uncontrolled manner. The assembled BNG is mounted with the shield onto the setup, thus the shield is always grounded.

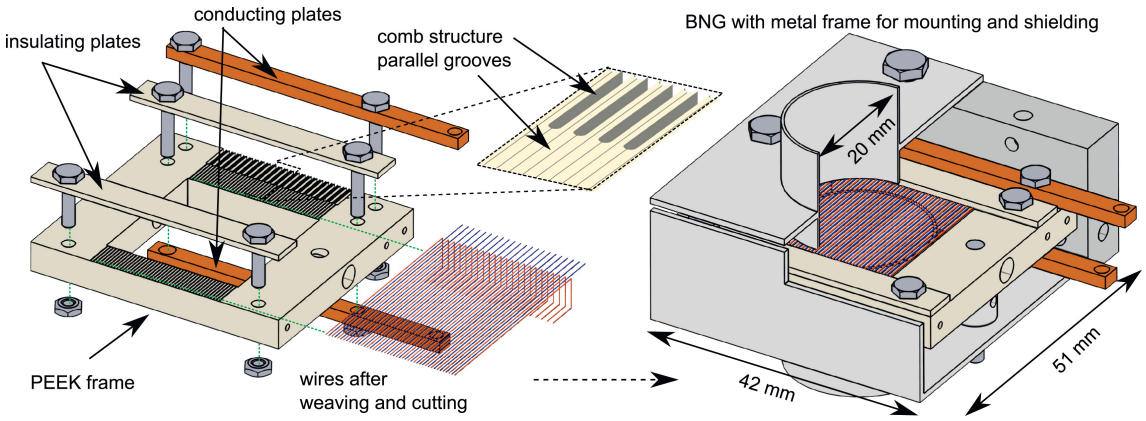


**Figure 14:** Design and schematic assembly of the Bradbury-Nielsen gate (BNG) proposed by R.N. Wolf et al.[13]. Figure taken from [13].

The BNG's PEEK frame and its metallic inner- and the outer shield have been fabricated at Max Planck Institute for Nuclear Physics in Heidelberg (see appendix 7 for detailed technical drawings).

## 4.2 Ultra-high vacuum cleaning

As the illustration of the BNG in figure 14 shows, the BNG consists of several different parts. Before starting the assembly of the BNG, these parts must be subjected to an ultra-high vacuum cleaning (UHV cleaning). It is indispensable to follow a thorough cleaning procedure to later achieve ultra-high vacuum conditions in the setup (pressure below $1 \times 10^{-8}$ mbar). UHV cleaning is a rigorous and tedious multi-step process. A more general procedure is described below:

1. Each part is cleaned first with soapy water and appropriate brushes to remove any grease and oils.
2. The parts are placed in a glass bottle filled with soapy water which is then placed in a sonicator for the appropriate time for each material, e.g. stainless steel for 30 min, but aluminum for only 10 min to avoid oxidation.
3. Parts are rinsed with tap water and placed in the sonicator again in a glass bottle filled with distilled water under the same time conditions as in step 2.
4. Parts are rinsed with distilled water multiple times and then placed in the sonicator in a glass bottle filled with isopropanol for 5 min.

After this procedure, the parts are considered as UHV clean and can be used for a UHV assembly where they will be only touched with clean gloves. Wearing clean gloves is essential when assembling for UHV purposes. As soon as the gloves touch something that does not meet the required cleaning standard, they are no longer considered clean and must be replaced. Therefore, clean gloves must be worn at all times during the cleaning process and afterward for the UHV clean assembly.

## 4.3 Weaving the wire onto the frame

First step in the UHV clean assembly is to weave the wire onto the PEEK frame. This must be done with high precision and this on a micron-level. It is extremely difficult to implement and only with the help of a weaving device possible which can maintain a constant wire tension. This is crucial as the BNG's performance rests on having an equidistant, parallel wire grid perpendicular to the beam axis. Applying inconsistent tension on such a thin wire, roughly the size of a human hair, would produce irregularities in the wire grid. Ions passing through these spots could be deflected with a smaller deflection angle or in undesired directions. In the next section 4.4 weaving devices are introduced which enable such a precise weaving procedure.

## 4.4 Overview of weaving devices

In this work, a weaving device was developed using components already available in the laboratory and 3D-printed parts. This self-developed device is shown in figure 15 on the left. On the right in figure 15 a weaving device is shown designed and assembled by O.K. Yoon et al. [11]. Hereby, tension is created by a weight (D) hanging on the wire between the wire spool (A) and the pulley wheel (E) that guides the wire into the grooves of the frame (B). When the handle is turned (c), the frame rotates and the spool unwinds as it is connected to the pivot axle via a timing belt (F) [11].

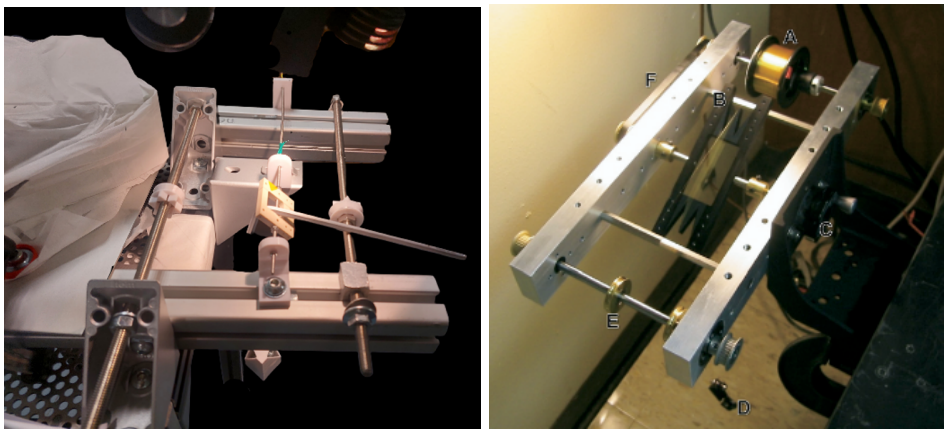


(a) self-developed weaver: designed and assembled out of parts already available parts in the laboratory and 3d-printed components.

(b) weaver designed and assembled by O. K. Yoon et al. [11].

**Figure 15:** Auxiliary devices for weaving the wire onto the frame of the BNG.

Weaving devices like those of O.K. Yoon et al. [11] serve as inspiration for the weaving device shown in the figure 15 on the left. The main challenge is to design pieces that perform the same tasks as those of the inspiratory devices but are made of accessible materials instead. Those materials are either already available in the lab and can be repurposed for the time it takes to assemble the BNG or are 3D-printed exactly for this purpose.

The elements of the self-developed weaving device are discussed in detail in the following section 4.5 in terms of design choice and availability in the laboratory. It is first described how to apply the necessary constant tension and precisely guide the wire into the grooves of the PEEK frame and then how the device can be used to rotate the BNG for weaving, but also to prevent it from unwinding.

## 4.5 Designing and building the weaving device

The individual components are discussed in more detail in this section. For this purpose, they are shown in close-up in the figure 16. The wire runs from the spool (A) under the adjustable weight (B) onto the guide wheel (C) which guides the wire into the grooves of the BNG's PEEK frame (D).

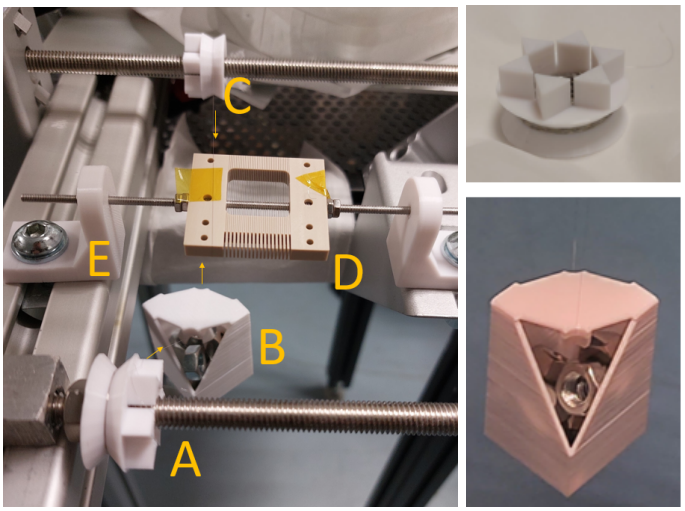


(a) close up on main elements (b) Spool and basket

**Figure 16:** Close up on the main elements of the weaver: spool (A), basket with nuts as a modifiable weight (B), guiding wheel (C), and BNG frame (D), support structure for the M2.5 rod as rotation axis (E).

To test the appropriate tension for the 50 $\mu$m- wire, the idea was to use an adjustable weight. So, a small basket was designed and 3D-printed to place light weights in it. By placing the desired number of weights the weight could be adjusted in a fast way during a test assembly. With a total weight of 70.93 g, a good enough tension was achieved without risking breaking the wire. The basket which is shown in figure 16 is designed in a way that the wire can slide underneath the plastic wheel so the frame's grooves are distributed on a larger wire section and the wire does not slide over any sharp edge. The wheel of the basket is designed to hold the wire in place and help guide the wire. That is why both edges of the wheel converge with a steep inclination to the center to create a small groove in which the wire can be placed similarly to the spool (A) or the guiding wheel (C) in figure 16.

In order to complete the vacuum clean assembly, it is important that the weaver offers freedom of rotation if necessary, but also prevents it if it is not desired. To achieve that the holes on the side of the BNG are slightly bigger (M3) than the diameter of the rod (M2.5). So, the BNG can be rotated easily on the threaded rod which functions as a rotation axis. If necessary, the PEEK frame can be fastened with two nuts countered against each other on each side of the PEEK frame as shown in figure 16. For additional security, an Allen key can be used to prevent the frame from unwinding as shown in figure 15. To hold the M2.5 rod in place, two support structures (E), shown on both sides of the BNG in figure 16, were designed and 3D-printed. It was necessary to mount them near the BNG on both sides to prevent a tumbling motion of the BNG as the rod was not completely straight.

The guiding wheel (C) shown in figure 16 has two functions. The first function is that it protects the wire from any sharp edges. Just sliding the wire over the rod could damage the surface of the wire and a smooth wire surface is needed to reduce the chance of sparking when a high voltage

is applied between the two separate wire sets. The second function is that it guides the wire into the frame's grooves (see figure 17). The 3D-printed part of the guide wheel was designed with a hole in the center to fit preciously over an M8 nut. These two components were glued together for reasons of stability. The nut could be moved along the M8 threaded rod during the weaving process. After each turn of the BNG, the nut had to be turned slightly by hand, i.e. moved slightly from right to left along the threaded rod. This simplified and sped up the whole weaving process as it was easy to go from groove to groove without having to reposition the wire by hand after each revolution.

The spool was made the same way as the guide wheel, only with larger dimensions to have enough space for winding an amount of wire for approximately four to five BNGs on it. To prevent the wire from unwinding because of the weight hanging onto it, the spool, more specifically the nut, was countered against another M8 nut as shown in figure 16. Clamping of the M8 rods was provided among others with oversized washers and nuts with a clamping part.

The woven PEEK frame is presented in figure 17. As shown in the microscopic view, the wire grid is smooth and equidistant, and it is precisely positioned within the groove structure of the frame. As a result, this self-developed weaving device meets the in section 4.3 desired performance requirements and hence represents an alternative solution to existing devices. The benefits of the self-developed weaving device, shown in figure 16, are that it may be easily rebuilt using widely available materials. It is simple to operate, and the weaving process takes between one and two hours.

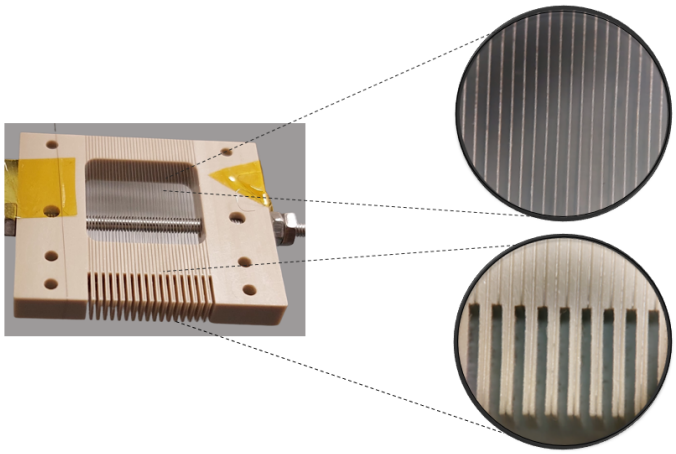

**Figure 17:** Ultra-high vacuum clean assembly of the BNG: wire is weaved on the BNG; microscope perspective equally distanced wires; small grooves on top and bottom for separating the two wire sets. PEEK frame designed by R.N. Wolf et al. [13] and fabricated at Max Planck Institute for Nuclear Physics in Heidelberg (see appendix for detailed technical drawings 7).

## 4.6 Mechanical integrity and electrical connections

The next step in the UHV clean assembly is to provide mechanical stability and, later, an electrical connection between the two wire sets generated after the wires are cut. For this, two insulating teflon plates and two copper plates were glued with non-conductive [2] or conductive [3] ultra-high vacuum-friendly adhesive to the PEEK frame to secure the wires onto the frame for long-term mechanical integrity and to electrically contact every second wire with each other. To harden and outgas the glues, the BNG shown in figure 18 was inserted into the small vacuum chamber shown in figure 19. This small chamber was assembled for baking out the BNG. It is clamped onto a supporting structure so that heating tape can be easily wrapped around the chamber. A temperature of more than 100 °C was not surpassed during baking to avoid melting any adhesive. If the conductive glue melts, it might connect the two wire sets, making the BNG unusable.

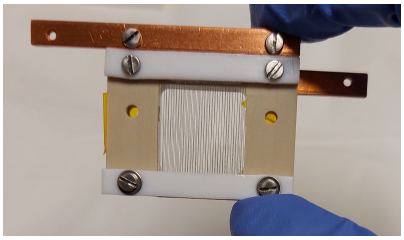

**Figure 18:** BNG after insulating and conductive plates are glued on the frame and after it was baked out.

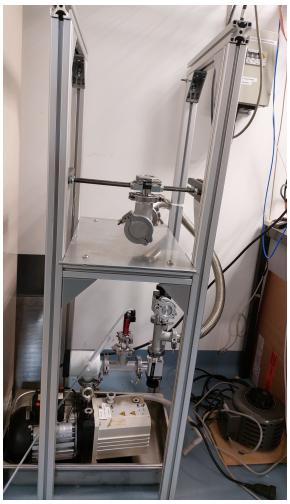

**Figure 19:** Self-assembled mini vacuum setup including a small chamber, hose, venting valve, gauge, valve, and a scroll pump. Clamped for winding the heating tape over the camber for the bake-out.

After hardening the glues, the wires were cut at the backside of the PEEK frame to enable two sets of wires which are electrically disconnected from each other. As shown in figure 18 the wires of the bottom wire set (according to 17) are clamped and connected with each other through the copper plate at the frame's front side. The wires going through the upper grooves (according to 17) are clamped and connected at the backside of the PEEK frame. So, the copper plates are not in contact with each other.

[2] vacuum epoxy adhesive from Torr Seal
[3] silver based epoxy adhesive from Farnell

After checking the BNG's electrical connections with a multimeter, the inner- and outer shields were attached to the frame using a cut-to-size M2.5 rod and spring washers to prevent the fasteners from loosening due to vibration in the ultra-high vacuum setup. In order to install the assembled BNG into the setup, a support structure had to be designed and fabricated, which is shown in figure 20 or in more detail in figure 21. This allows the BNG to be mounted on an actuator so that the position of the BNG can be changed along the actuator axis. Thus, the BNG can be placed in the beam line or retracted if necessary. The development of the support structure is described in the following section 4.7.

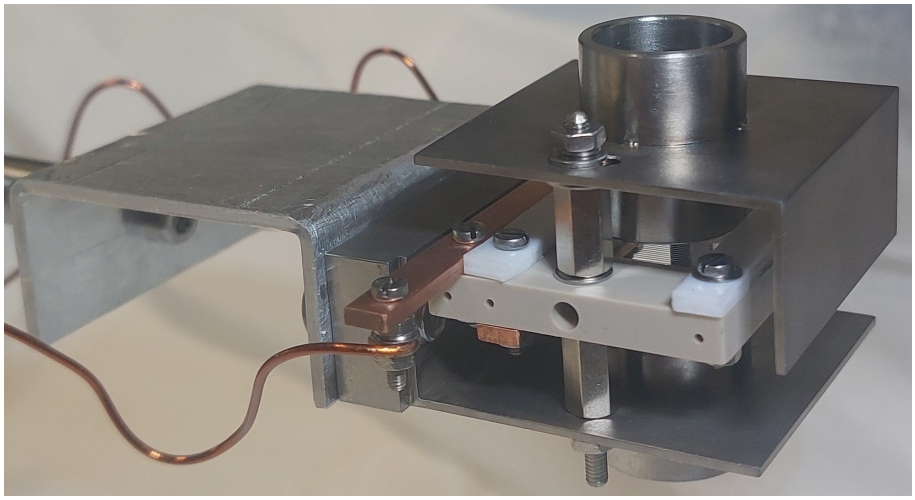

**Figure 20:** BNG mounted on actuator via support structure, ready to install. PEEK frame, inner and outer shielding designed by R.N. Wolf et al. [13] and fabricated at Max Planck Institute for Nuclear Physics in Heidelberg (see appendix 7 for detailed technical drawings)

## 4.7 Building a self-developed support structure for installing the BNG

At the top of the actuator shaft, there is an M4 hole. Two M6 mounting holes are spaced apart on the BNG's outer shield. The support structure was made out of a thin aluminum plate because of how light it is. In order to place the BNG into the beamline, the support structure had to be bent twice through a crucial 90 degrees. The M4 hole must be precisely in the center of the two M6 holes since the actuator only has one degree of freedom and its shaft is centered in the beamline. The BNG must be precisely positioned in the ion beam path because the opening of the inner- and outer shield is only 15 mm wide. Otherwise, the ion beam width could significantly reduce the transmission. The simulated ions in figure 7, however, are more spread in the horizontal direction, which is also where the actuator offers its degree of freedom. In the following section 5, the right actuating position is determined.

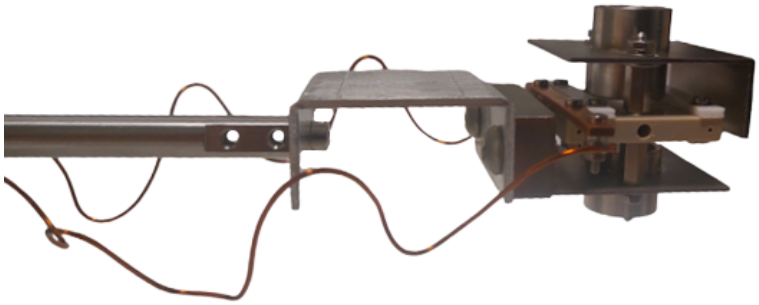

**Figure 21:** Self-built support structure is mounted with an M4 screw on the actuator shaft and connected to the BNG with two M6 screws.

# 5 Installing and commissioning the BNG

The actuator shaft with the mounted BNG was reinstalled into the ultra-high vacuum setup at the position for which the feasibility study was performed in section 3. In this section, it will be determined if the installed BNG can fulfill the performance requirements defined in section 3:

1. Above 90% transmission in BNG's transparent state
2. 0% transmission in BNG's deflecting state
3. Above 99% purification of the selected isotope
4. Minor influence on the selected ions motion which means fast switching between BNG's deflection and transparent mode

## 5.1 Experimental foundation

The counts represent how many ions the detector registers in total. Each measurement run is carried out for at least 100 cycles. Each cycle represents the process of performing the entire measurement operation (accumulation, bunching, passage, or non-passage through BNG, and measurement at detector), hence one cycle is the process performed for one ion bunch. The count rate R for one measurement run is given by the ratio of the total counts N registered and the number of cycles C performed:

$$R = \frac{N}{C}. \tag{11}$$

N and C are statistically independent. Thus, the squared relative uncertainty on the ratio of two measurements is the squared sum of their relative uncertainties which arises as a special case from the Gaussian error propagation law. So, the statistical error of the count rate R can be calculated as follows:

$$\left(\frac{\sigma_R}{R}\right)^2 = \left(\frac{\sigma_N}{N}\right)^2 + \left(\frac{\sigma_C}{C}\right)^2. \tag{12}$$

However, the uncertainty for the number of cycles can be assumed to be zero since it is the same as counting the number of repetitions ion bunches are sent towards a detector. With $\sigma_C = 0$ the formula for determining $\sigma_R$ reduces to:

$$\sigma_R = R \cdot \frac{\sigma_N}{N} = \frac{\sigma_N}{C}. \tag{13}$$

Since the statistics of counting measurements follow Poisson statistics, the statistical error of the total counts N is given by:

$$\sigma_N = \sqrt{N}. \tag{14}$$

With this, the statistical error of the count rate R can be calculated with this end formula:

$$\sigma_R = \frac{\sqrt{N}}{C}. \tag{15}$$

## 5.2 Determination of BNG's measurement position

As stated previously in section 4.7, it is necessary to determine the BNG's right actuating position first. For this, the following measurement conditions are established: The continuous ion beam of chlorine isotopes ($^{35}$Cl and $^{37}$Cl) is trapped and bunched in the Paul trap. After being emitted the bunched ion beam enters the BNG area. If the BNG is in the correct actuating position, the ions pass with high transmission through the transparent BNG and are detected at the detector

behind the MR-ToF device. [4]

The count rate was determined while the BNG was moved further and further into the chamber. The structure of the graph in figure 22 can be explained as follows: If the actuator shaft is moved 70 mm into the chamber, the BNG is not yet in the ion beam area. Therefore, the count rate is roughly as if the BNG was fully retracted, which corresponds to an actuator position of 0 mm. After the 70 mm position, the count rate drops drastically to 0 $\frac{\text{counts}}{\text{cycle}}$. This is caused by the front part of the metallic shield of the BNG shown in figure 21 when it blocks the ion beam. As the count rate increases again, the shield opening becomes more and more centered in the ion beam and remains centered for the high count rates between the actuator positions 95 mm and 102.5 mm. When the count rate drops again, the shield starts blocking the beam again. The mean value of 99.8 mm for the actuator position was calculated from the five data points in figure 22 where the count rate is high. Therefore, 100 mm was taken as the optimal operating position of the BNG.

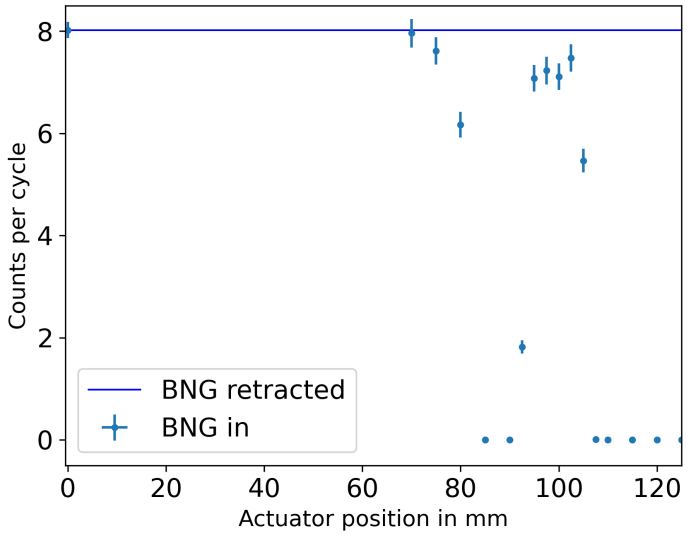


**Figure 22:** Count rate (counts per cycle) dependent on BNG's position on the actuator axis: The BNG is in its transparent state and the statistical uncertainty of the count rate is determined as previously explained in section 5.1.

## 5.3 Determination of BNG's transmission in transparent state

To test whether the BNG meets the performance criteria of over 90% transmission in its transparent state, two measurement runs with a minimum of 100 cycles per measurement run were performed, one with the BNG in actuating position and one immediately after with the retracted BNG. This procedure is performed four times to ensure that the slightly unstable ion beam is not significantly reducing transmission at any time. Because of this, the third and fourth repetitions in table 3 are performed about an hour later than the first and second.

The statistical uncertainty of the count rates in table 3 is calculated in the same way as stated previously in section 5.1. Because the measured count rates of different experimental runs are statistically independent, the statistical uncertainty of the transmission is determined using Gaussian error propagation.

[4] For illustration purposes, figure 3 shows a schematic overview of the MIRACLS setup.

**Table 3:** BNG's transmission in transparent mode, i.e. two grounded wire sets, was determined four times

| Number of repetitions | Count rate (BNG in) | Count rate (BNG retracted) | Transmission |
|---|---|---|---|
| 1 | 11.28 ± 0.17 | 11.31 ± 0.17 | 99.7% ± 2.1% |
| 2 | 10.53 ± 0.22 | 11.01 ± 0.27 | 95.7% ± 3.1% |
| 3 | 11.68 ± 0.33 | 11.85 ± 0.29 | 98.6% ± 3.7% |
| 4 | 11.33 ± 0.28 | 12.11 ± 0.29 | 96.1% ± 3.3% |

As shown in table 3, the transmission of the BNG is way above the desired 90%. Thus, the BNG fulfills the performance requirement in its transparent state.

## 5.4 Determination of BNG's transmission in its deflecting state

The second performance requirement defined in section 5 is to achieve 0% transmission when the BNG is in its deflecting state. For this, the appropriate operation voltage is determined in this section. Measurement runs are performed depending on the voltage applied to the BNG. With a sufficiently high voltage, the deflection angles should be large enough to prevent ions from entering the MR-ToF device and thus being detected by the detector behind it.

The count rate is depicted in figure 23 as a function of the voltage applied to one wire set of the BNG while the other is grounded. As shown in figure 23, the count rate is higher for lower voltages up to around 150 V than when the BNG is in its transparent state which corresponds to 0 V applied. This can be explained by the ion beam simulation 7 in section 3.2 which demonstrates the large ion beam width. According to this simulation, the ion beam width is larger than the diameter of the opening of the MR-ToF. Ions at the edge of the distribution, which would normally not enter the apparatus, are deflected with a small angle into the opening.

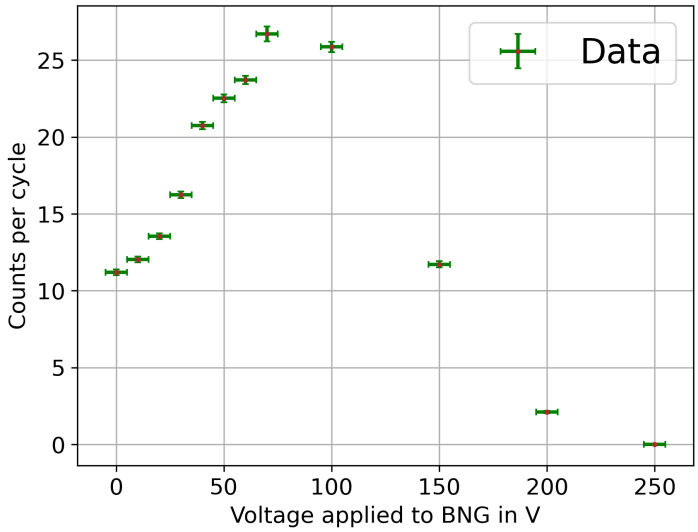


**Figure 23:** Count rate as a function of the voltage applied to one wire set of the BNG.

Figure 23 shows that the count rate disappears when a voltage of at least 250 V is applied to the

BNG. Thus, the ions are deflected at a large enough angle by the BNG not to be registered by the detector. So, the BNG also meets the second performance requirement which is to achieve 0% transmission in its deflecting state.

## 5.5 Isotope purification performance and influence on the selected ion's motion

### 5.5.1 Maximum purification determination

This section evaluates the ability of the BNG to effectively separate the $^{35}$Cl and $^{37}$Cl isotopes. To this end, measurement runs are performed while changing the BNG's switching start time in steps of 100 ns (or 50 ns).

As discussed in section 3.4, a symmetric switch is crucial for isotope shift measurements. A fast rise and fall time of the voltage pulse and a time window of $\Delta T \approx 400$ ns are required for ideal switching conditions. However, the minimum time window $\Delta T$ the available switches can output is about 730 ns, as shown in sub-figure (a) of figure 24. Two switches with different rise and fall times of voltage pulses they can generate are shown in sub-figure (b) of figure 24. The rise time is determined by the time it takes for the voltage pulse to change from 10% to 90% of its maximum baseline value measured from ground. The faster switch has a fall time of 40 ns while the slower switch has one of 120 ns.

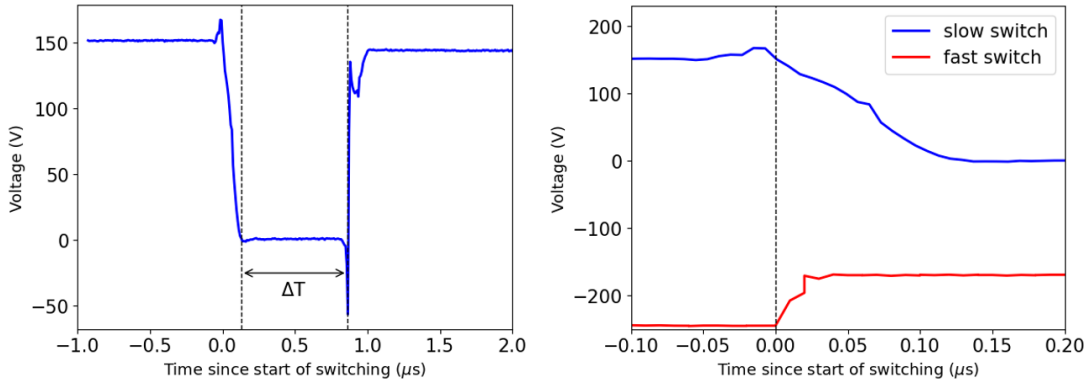


(a) BNG is in its transparent state for a time window $\Delta T \approx 0.73\,\mu$s.

(b) Comparison between rise and fall time of fast and slow switch.

**Figure 24:** Available switches for switching the BNG: Voltage pulse output by the slower switch (a) and rise and fall time comparison of the fast and slow switch (b). (The measurement of the voltage pulse and the rise and fall time of each switch is not performed in this work because the prerecorded data was already available for use. The magnitude of voltage does not represent the one used in the following measurements.)

The rise and fall time of the voltage pulse applied to the BNG can have an additional influence on the ions' motion because ions can be deflected at different angles by a rising or falling voltage pulse. The longer the rise and fall time, the greater the influence is expected to be. For comparison, the following measurements are performed with both switches.

Figure 25 shows the isotope ratios change depending on the time the slow switch receives the signal to switch the BNG and figure 26 shows the same for the fast switch. In both figures, there are switching start times where the count rate for one isotope is high and at the same time so low for the other isotope that it is nearly vanishing. For instance, a switching start time between 5.3 $\mu$s to 5.5 $\mu$s seems good for using the slower switch to measure $^{35}$Cl with high purification as it can be seen in figure 25. For a switching start at 5.4 $\mu$s, $^{35}$Cl is measured with 99.94% $\pm$ 0.03% purification which exceeds the purification performance requirement of 99%.

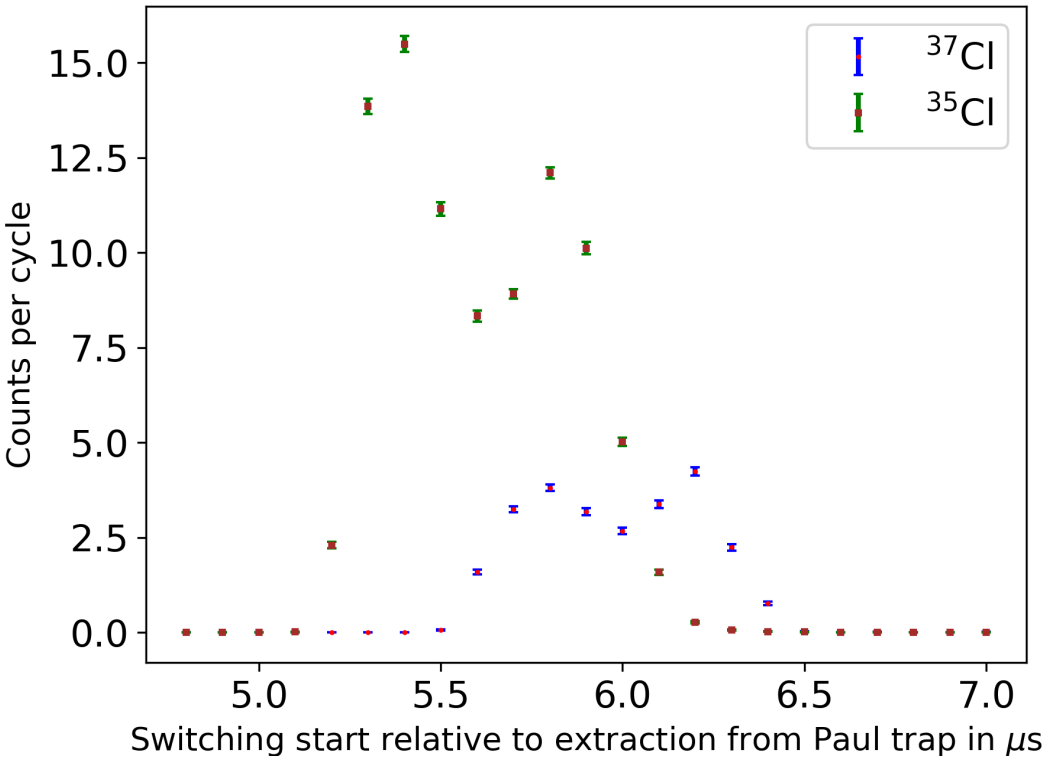


**Figure 25:** Count rate of $^{35}$Cl and $^{37}$Cl plotted over time when the slow switch receives the signal to switch the BNG from deflection to transmission mode: The applied voltage on one wire set is always 500 V except for a small time window $\Delta T \approx 0.73\,\mu$s where it is switched to ground potential, while the other wire set is always grounded.

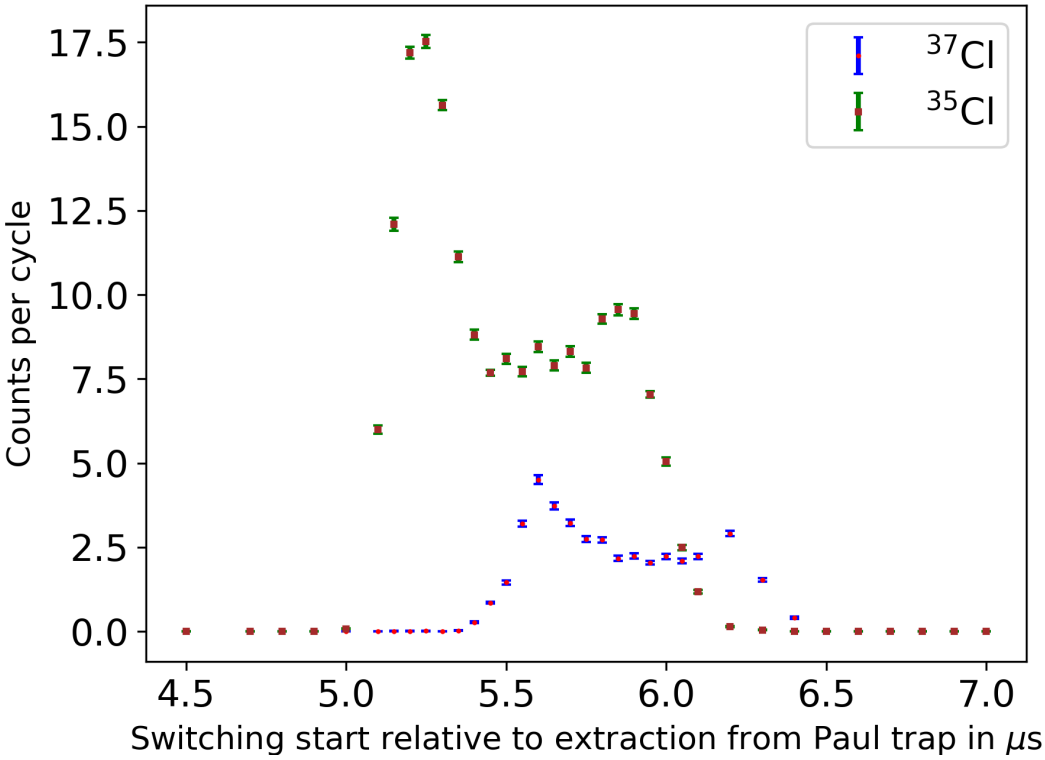


**Figure 26:** Count rate of $^{35}$Cl and $^{37}$Cl plotted over time when the fast switch receives the signal to switch the BNG from deflection to transmission mode: The applied voltage on one wire set is always 500 V except for a small time window $\Delta T \approx 0.7\,\mu\text{s} - 0.8\,\mu\text{s}$ where it is switched to ground potential, while the other wire set is always grounded.

### 5.5.2 Effect of different switching conditions on isotope purification and influence on selected ion's motion

Although for a switching start after 5.4 $\mu$s with the slower switch the contamination of $^{37}$Cl is less than 1%, it turns out that the BNG has an impact on the selected ions' motion. This can be seen from the shape of $^{35}$Cl distribution in figure 27. The cause is that the rise time and the time window $\Delta T \approx 0.73\,\mu$s of the switch are too long. As discussed in section 3.4, the time window needs to be halved to effectively separate the isotopes with above 99% purification and without influence on the selected ion's motion at the same time. During the 120 ns rise time of the voltage pulse output by the slow switch, the ions of the selected isotope can be deflected at different angles by the rising voltage pulse.

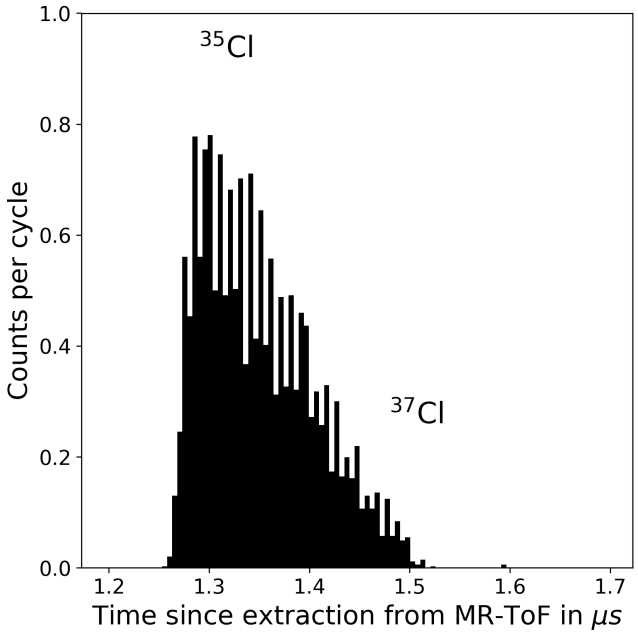


**Figure 27:** Isotope distribution when the slower switch starts switching the BNG from its deflection to its transmission mode after 5.4 $\mu$s since ions are extracted from the Paul trap.

Figure 28 compares the $^{35}$Cl distributions of both switches with each other. It can be seen that the slower switch ( sub-figure (b)) has a bigger influence on the movement of the ions than the faster switch ( sub-figure (c)) because the tail of the $^{35}$Cl peak is more prominent. In figure 28 a reference measurement can be seen with the BNG in its transparent state. Here, also the distributions do have tails and do not have an ideal Gaussian shape. Thus, the asymmetric shape is not only an effect of the BNG. Comparing a switching start at 5.40 $\mu$s ( sub-figure (c) of figure 28) with the reference sample (graph (a)), it can be seen that apart from a longer tail in sub-figure (c) the two $^{35}$Cl distributions are quite similar in height and shape. The contamination with $^{37}$Cl at a switching start of 5.4 $\mu$s of the fast switch is 3.07% $\pm$ 0.44%. Thus, with the fast switch, 96.93% $\pm$ 0.44% purification is achievable with little impact on the $^{35}$Cl distribution.

By comparing the $^{35}$Cl distribution at a switching start of 5.40 $\mu$s with a switching start at 5.45 $\mu$s, it is clearly visible how a slightly later switching start of 50 ns reduces the tail of the $^{35}$Cl distribution, but at the same time increases the contamination with $^{37}$Cl. The purification is then only 88.93% $\pm$ 0.40%.

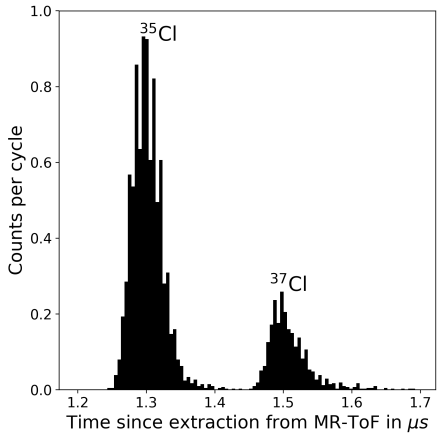


(a) Reference: BNG in transparent mode. (no switching)

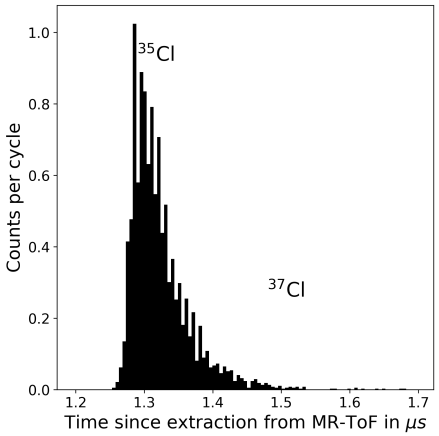


(b) Slow switch starts switching after 5.5 $\mu$s.

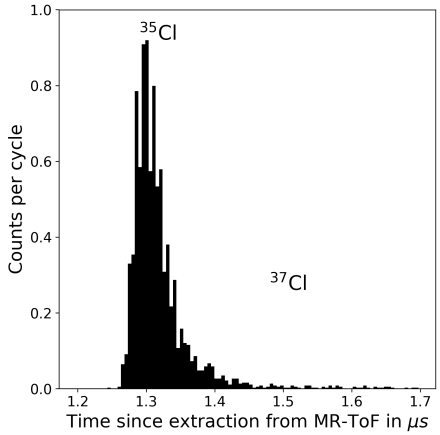


(c) Fast switch starts switching after 5.4 $\mu$s.

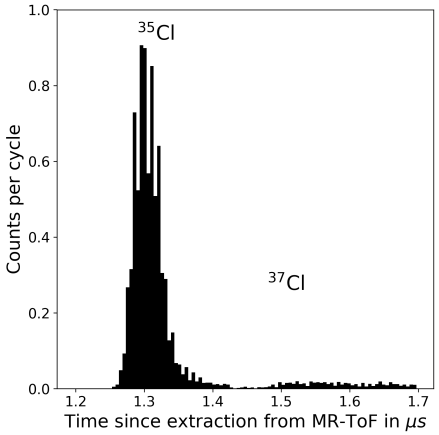


(d) Fast switch starts switching after 5.45 $\mu$s.

**Figure 28:** Isotope purification of $^{35}$Cl using the BNG: Isotope distributions are shown at varying switching start times of the two switches (fast and slow).

As a result, high purification can be achieved with the installed BNG while having little impact on the ions' motion of the selected isotope bunch. A switch capable of producing voltage pulses with a reduced time window $\Delta T$ is required to improve the purifying performance while still ensuring low impact on the selected ions' movement.

# 6 Conclusion

Atomic theory models of multi-electron systems are in need of new stringent tests of their predictions. Isotope shifts in the electron affinity are highly impacted by electron correlations and thus provide excellent tests for these theories. However, experimental determination of these shifts is rare in literature due to sensitivity limitations. However, MIRACLS' experimental technique can boost signal sensitivity by orders of magnitudes.

For a precise measurement of the isotope shift, each isotope has to be measured independently with ideally less than 1% contamination of the other one. To not introduce new uncertainties to the measurement, the selection method should not influence the selected ions' motion. Thus, a fast and sharp selection method is required.

For this reason, a Bradbury-Nielsen gate (BNG) has been assembled in this thesis. Additionally, a new method has been introduced in this work on how to quickly design and build an auxiliary device for the assembly with components made of accessible materials. This can make the overall assembly faster and less time-consuming.

Lastly, it has been demonstrated in this work that the BNG can achieve over 99% isotope purification while simultaneously exceeding the required transmission of 90%. It is also possible to achieve a selection of the $^{35}$Cl isotope with a minor influence on the ions' motion and simultaneously a relatively high purification of 96.93% $\pm$ 0.44%. Thus, the assembled BNG fulfills all of its performance requirements and can be used for MIRACLS' future isotope shift measurements.

To fully exploit the advantages of a BNG for the isotope shift measurement, a switch that can provide a smaller time window is required. There it is essential that each ion bunch is cut symmetrically around its center and that both isotope bunches are cut identically to avoid introducing any new energy shifts between the isotopes.

# References


[1] Pegg, David J. ; Drake, Gordon W. F.: Handbook of Atomic, Molecular, and Optical Physics. In: *Springer New York* edition number 1 (2005), S. 891–892

[2] Pegg, David J.: Structure and dynamics of negative ions. In: *Rep. Prog. Phys* 67 (2004), S. 857

[3] King, W. H.: *Isotope Shifts in Atomic Spectra.* 1. SPRINGER SCIENCE+BUSINESS MEDIA, LLC, 1984

[4] Campbell, P. ; Moore, I.D. ; Pearson, M.R.: Laser spectroscopy for nuclear structure physics. In: *Progress in Particle and Nuclear Physics* 86 (2016), S. 127–180

[5] Cheal, B. ; Cocolios, T. E. ; Fritzsche, S.: Laser spectroscopy of radioactive isotopes: Role and limitations of accurate isotope-shift calculations. In: *Phys. Rev. A* 86 (2012), S. 042501

[6] Berzinsh, U. et a.: Isotope shift in the electron affinity of chlorine. In: *Physical Review A* 51 (1995)

[7] Wigner, Eugene P.: On the Behavior of Cross Sections Near Thresholds. In: *Phys. Rev.* 73 (1948), S. 1002

[8] Farley, John W.: Photodetachment cross sections of negative ions: The range of validity of the Wigner threshold law. In: *Phys. Rev. A* 40 (1989), S. 6286

[9] Maier, F. M.: *Highly-sensitive photodetachment spectroscopyin an MR-ToFdevice.* `https://indico.cern.ch/event/1104299/contribution/5055352/attachments/2533235/4359162/EuNPCnegions.pdf`, 2022. – Accessed: 2023–01-23

[10] Carette, T ; Godefroid, M R.: Isotope shift on the chlorine electron affinity revisited by an MCHF/CI approach. In: *Journal of Physics B: Atomic, Molecular and Optical Physics* 46 (2013), Nr. 9

[11] Yoon, O.K. et a.: Simple template-based method to produce bradbury-nielsen gates. In: *J Am Soc Mass Spectrom 18* (2007)

[12] Bradbury, N. E. ; Nielsen, R. A.: Absolute values of the electron mobility in hydrogen. In: *Physical Review , 49(5):388* (1936)

[13] Wolf, R.N. et a.: On-line separation of short-lived nuclei by a multi-reflection time-of-flight device. In: *Nuclear Instruments and Methods in Physics Research Section A: Accelerators, Spectrometers, Detectors and Associated Equipment* (2012)

[14] Weinkauf, R. et a.: Laser Tandem Mass Spectrometry in a Time of Flight Instrument. In: *Zeitschrift für Naturforschung A* 44 (1989), Nr. 12, S. 1219–1225

[15] Brunner, T. et a.: A large Bradbury Nielsen ion gate with flexible wire spacing based on photo-etched stainless steel grids and its characterization applying symmetric and asymmetric potentials. In: *International Journal of Mass Spectrometry* 309 (2012), S. 97–103

[16] Bethe, H.: Über den Durchgang von Kathodenstrahlen durch Gitterförmige Elektrische Felder. In: *Z. Physik 54, 703–710* (1929)

[17] Yoon, O.K. et a.: Duty cycle and modulation efficiency of two-channel hadamard transform time-of-flight mass spectrometry. In: *J Am Soc Mass Spectrom 16* (2005)

[18] Manura, Dahl D. D.: *SIMION (R) Version 8.1 User Manual.* `https://simion.com/`. – Last accessed June 5th 2023

[19] Maier, F.M. et a.: Simulations of a proof-of-principle experiment for collinear laser spectroscopy within a multi-reflection time-of-flight device. In: *Interact, 240: 54* (2019)

[20] Maier, Franziska M.: Laser Spectroscopy of Short-Lived-Radionuclides in an Ion Trap: MIRACLS' proof-of-principle experiment and the simulation of the future 30-keV MR-ToF device. In: *Master, Johannes Kepler University Linz* (2019)

[21] Kaia, N. et a.: A simple template-based transfer method to fabricate Bradbury–Nielsen gates with uniform tension for ion mobility spectrometry. In: *Review of Scientific Instruments* 85 (2014)

# 7 Appendix

A. Technical drawing of BNG's PEEK frame

B. Technical drawing of BNG's inner shielding

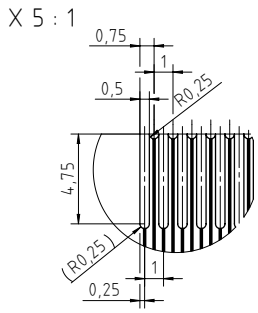


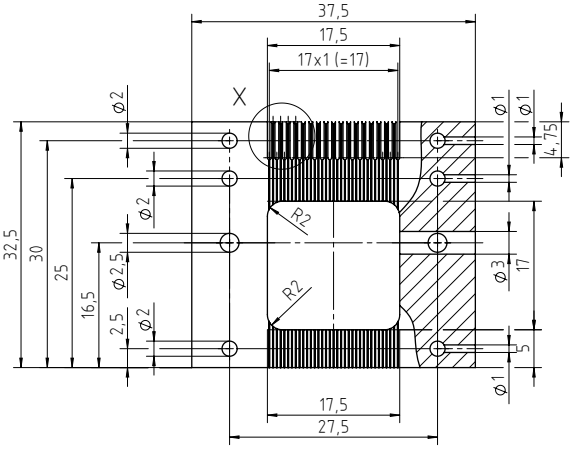


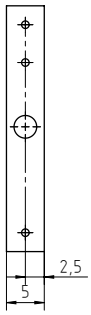


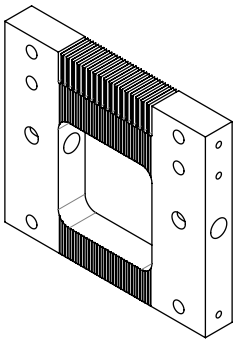

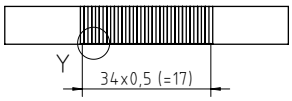


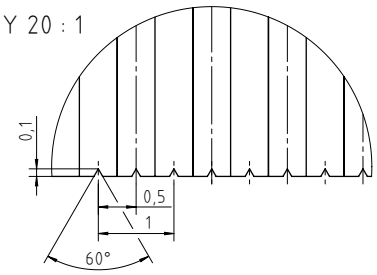


Teil ohne Öl/ Bohrwasser bearbeiten

Rz 16

-0,05 +0,05

| Rev | Änderung | Datum | Name | | |
|---|---|---|---|---|---|
| | | | | Maßstab: 2:1 | Metrisch |
| | | | | Format: DIN A3 | |
| | | | | Blatt: 1 von 1 | |
| | | | | Koordinator: Blaum | |
| | | | | Konstrukteur: Weißmann | |
| | | | | Zeichner: Weißmann | |
| | | | | Allgemeintoleranzen für Längen- und Winkelmaße, Form und Lage nach ISO 2768-mK<br>Werkstückkanten ISO 13715<br>Oberflächen nach ISO 1302 | |

Max-Planck-Institut für Kernphysik Heidelberg

Name:

Anzahl:

Komponenten-Status: FREIGABE

Spezifikation:

Material: PEEK (Polyetheretherketon)

Benennung: CERN - BNG__v3

Projekt: 001 - Abt. Blaum Allgemein

Freigabe: 09.08.22 Steinhauser

Revision:

Auftrag: | Kostenstelle: | Komponenten-Nr.: 029255.001

L:\EPDM\1\001\CAD Daten\029255 - 001

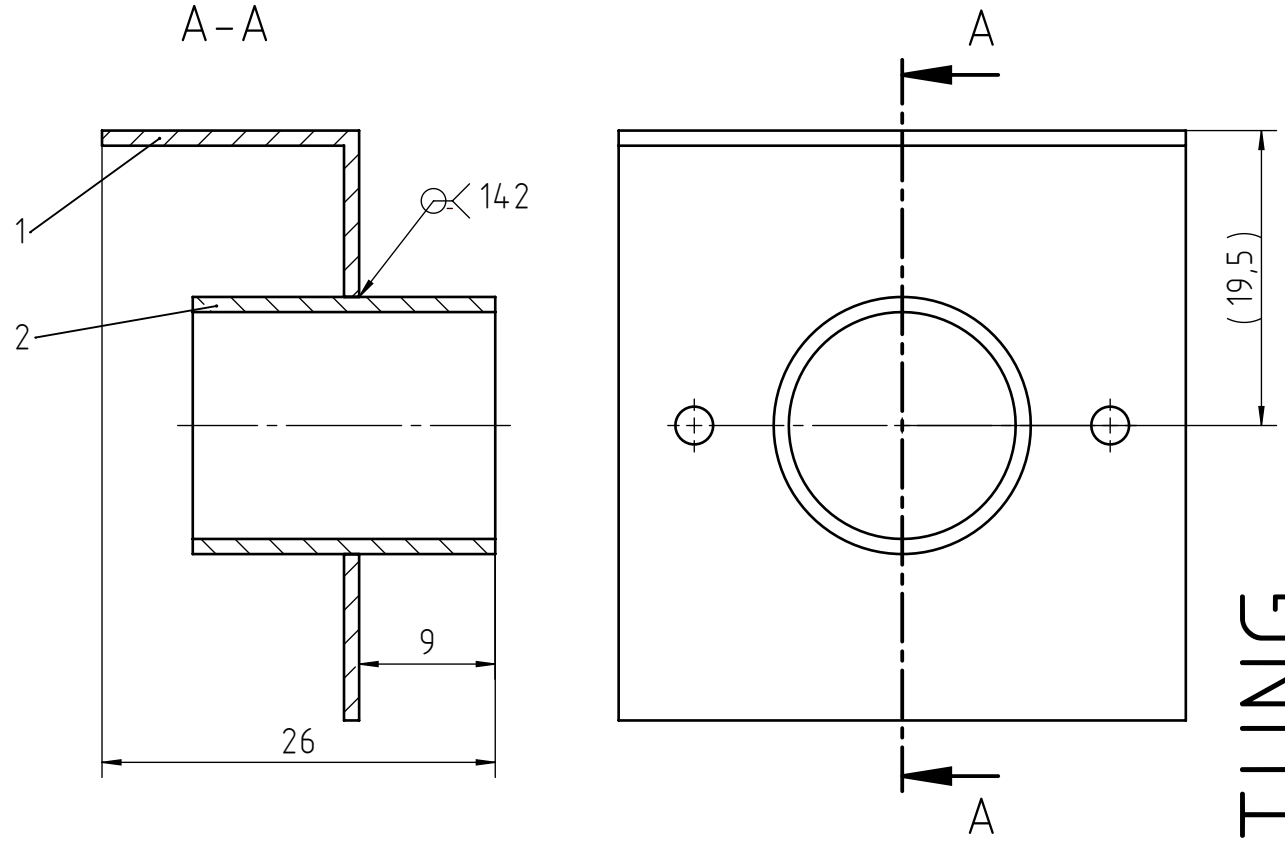


IN BEARBEITUNG

| Pos. | Nummer | Benennung | Anz. | Abmessung | Material | Anmerkung | Rev. |
|---|---|---|---|---|---|---|---|
| 2 | 029223.001 | CERN-BNG - Inner Shield Ring 1 - Rohr | 1 | Ø17 × Ø1 - L= 20 | 1.4301 (X5CrNi18-10) | | |
| 1 | 029222.001 | CERN-BNG - Inner Shield Ring 1 - Winkel | 1 | 37,5 × 39 × 17 | 1.4301 (X5CrNi18-10) | | |

| Rev | Änderung | Datum | Name |
|---|---|---|---|
| | | | |
| | | | |
| | | | |
| | | | |
| | | | |
| | | | |
| | | | |
| | | | |
| | | | |

Maßstab: 2:1
Format: DIN A4
Blatt: 1 von 1
Metrisch

Koordinator: Blaum
Konstrukteur: Stark
Zeichner: Weißmann

Allgemeintoleranzen für Längen- und Winkelmaße, Form und Lage nach ISO 2768-mK
Werkstückkanten ISO 13715
Oberflächen nach ISO 1302

**Max-Planck-Institut für Kernphysik Heidelberg**

Name:
Anzahl:

Spezifikation:
Material:
Benennung: CERN-BNG - Inner Shield Ring 1
Projekt: 001 - Abt. Blaum Allgemein

Komponenten-Status: IN BEARBEITUNG
Freigabe:
Revision:

Auftrag:
Kostenstelle:
Komponenten-Nr.: 029224.001

L:\epdm\1\001\cad daten\029224 - 001

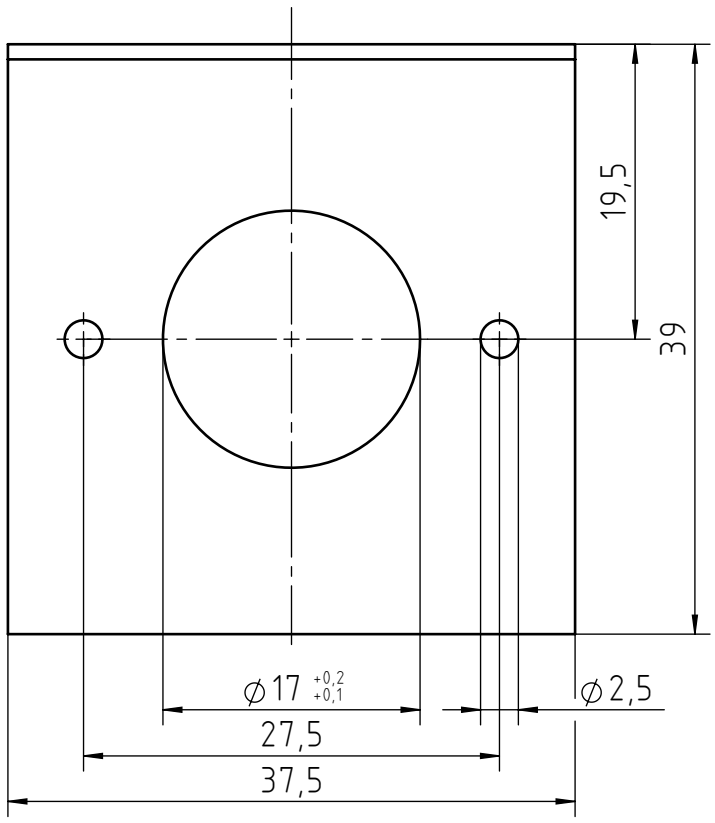


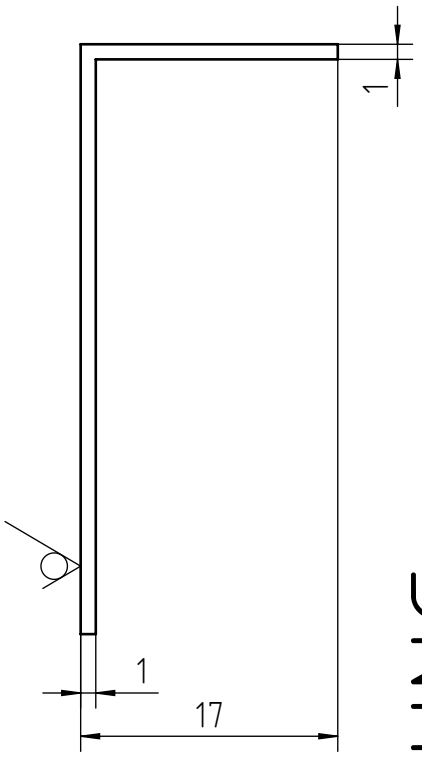


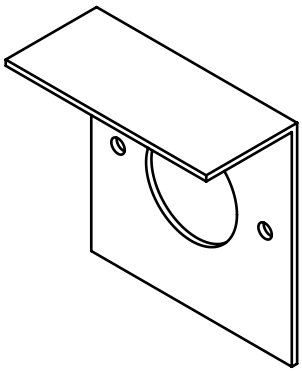

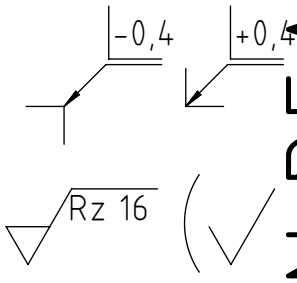


IN BEARBEITUNG

| Rev | Änderung | Datum | Name |
|---|---|---|---|
| | | | |
| | | | |
| | | | |
| | | | |
| | | | |
| | | | |
| | | | |
| | | | |
| | | | |

| | |
|---|---|
| Maßstab: | 2:1 |
| Format: | DIN A4 |
| Blatt: | 1 von 1 |
| Koordinator: | Blaum |
| Konstrukteur: | Stark |
| Zeichner: | Stark |

Metrisch

Allgemeintoleranzen für Längen- und Winkelmaße, Form und Lage nach ISO 2768-mK
Werkstückkanten ISO 13715
Oberflächen nach ISO 1302

**Max-Planck-Institut für Kernphysik Heidelberg**

Name:

Anzahl:

Komponenten-Status: IN BEARBEITUNG

Freigabe:

Revision:

Spezifikation:

Material: 1.4301 (X5CrNi18-10)

Benennung: CERN-BNG - Inner Shield Ring 1 - Winkel

Projekt: 001 - Abt. Blaum Allgemein

Auftrag:

Kostenstelle:

Komponenten-Nr.: 029222.001

L:\epdm\1\001\cad daten\029222 - 001

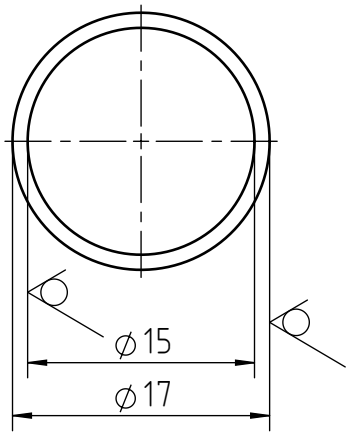


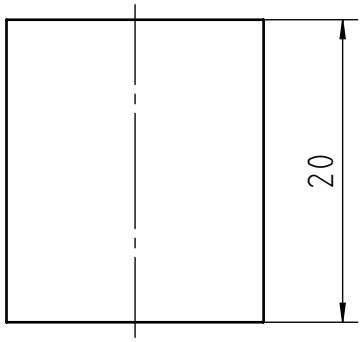


IN BEARBEITUNG

Rz 16

-0,2
+0,2

| Rev | Änderung | Datum | Name |
|---|---|---|---|
| | | | |
| | | | |
| | | | |
| | | | |
| | | | |
| | | | |
| | | | |
| | | | |
| | | | |

| | |
|---|---|
| Maßstab: | 2:1 |
| Format: | DIN A4 |
| Blatt: | 1 von 1 |
| Koordinator: | Blaum |
| Konstrukteur: | Stark |
| Zeichner: | Weißmann |

Metrisch

Allgemeintoleranzen für Längen- und Winkelmaße, Form und Lage nach ISO 2768-mK
Werkstückkanten ISO 13715
Oberflächen nach ISO 1302

**Max-Planck-Institut für Kernphysik Heidelberg**

Name:

Anzahl:

Komponenten-Status: IN BEARBEITUNG

Freigabe:

Revision:

Spezifikation:

Material: 1.4301 (X5CrNi18-10)

Benennung: CERN-BNG - Inner Shield Ring 1 - Rohr

Projekt: 001 - Abt. Blaum Allgemein

Auftrag:

Kostenstelle:

Komponenten-Nr.: 029223.001

L:\epdm\1\001\cad daten\029223 - 001